Distributed Economic Dispatch Algorithm With Quantized Communication Mechanism

Xiasheng Shi, *Member, IEEE*, Changyin Sun, *Senior Member, IEEE*, and Chaoxu Mu, *Senior Member, IEEE*

***Abstract*— Due to the limited bandwidth and energy of communication channels among agents in practical applications, the communication-efficient distributed optimization method has emerged as a pressing research topic in recent years. The distributed economic dispatch problem with restricted data communication/finite communication bandwidth is investigated in this study, where the communication among agents can be described as a strongly connected directed network. For this purpose, a robust push-pull distributed optimization algorithm with a dynamic scaling quantization mechanism is developed based on the gradient tracking technique. A novel surplus variable is designed to prevent the accumulation of quantization errors, and then, a heavy-ball momentum is introduced to speed up convergence performance. In addition, a linear convergence rate of the developed approach is deduced for the strongly convex and Lipschitz smooth cost function. Finally, we offer two instances for illustration.**

***Note to Practitioners*—This paper proposes a robust quantization-based algorithm for the economic dispatch problem, in which the broadcasting information is quantized before sending to its neighboring generators. Therefore, this method reduces duplicate transmission of agents and improves the use of communication resources. Furthermore, the developed method can be extended to similar constrained optimization problems, such as the resource allocation problem in wireless networks, and the network utility maximization problem in the Internet.**

***Index Terms*— Distributed economic dispatch, gradient tracking, heavy-ball momentum, limited communication bandwidth, smart grid.**

I. Introduction

IN RECENT years, the scheduling of power resources in the energy internet has received increasing attention. The economic dispatch problems (EDPs) are particularly crucial in energy management, which aims to construct a proper solver that enables the system to operate at the minimum power supply cost. Reasonable and practical completion of dispatch tasks dramatically enhances the economic benefits of the power grid. Therefore, a lot of centralized algorithms have been designed, including Lagrangian relaxation methods [1], dynamic programming-based methods [2], self-organized hierarchical particle swarm methods [3], mixed-integer linear programming methods [4], and others. However, these central methods require a central control agent to gather the information necessary for achieving the global optimal solution. Unfortunately, a small change may result in the failure of these central methods for large-scale systems [5]. In addition, with the development of the new power systems, various new energies, such as wind power generation and solar power, gradually occupy the leading position of installed capacity [6] and address the existing power gap and energy crisis. Thus, the large-scale emergence of distributed new energy has led to strong distributed characteristics in EDPs.

To address this issue in the energy internet, numerous excellent distributed procedures have been created by virtue of the consensus method in multi-agent systems, where each agent is equipped with functions like transmission, processing, and storage. Those methods can be divided into two types: Continuous-time and Discrete-time. Based on the differential equation theory, a number of continuous-time distributed economic dispatch algorithms have been designed in recent years. For example, with the help of the projection operator or the exact penalty function approach, many initialization-free distributed optimization schemes were designed and applied to the EDPs [7], [8]. Distributed control algorithms with exponential and asymptotical convergence rates were respectively designed for the EDP under non-local and local constraints by virtue of the saddle dynamics and the consensus structures, [9]. Furthermore, the saddle dynamics methods for box constraints in [9] were extended to more general local constraints in [10]. A novel newton-surplus-based method was designed in [11] to address the EDP for energy internet with information entropy in light of the Hessian matrix of the cost function. Similarly, an initialization-free Jacobi descent method was presented with the nonlinear scheme to tackle the EDP in the smart grid under DoS attacks [12]. To further accelerate the convergence speed, a distributed fixed-time optimization approach with continuous exponential consensus term was proposed in [13] to resolve the optimal resource management for microgrids. A similar fractional-order finite-time distributed optimization

Received 12 September 2024; accepted 22 October 2024. Date of publication 8 November 2024; date of current version 26 March 2025. This article was recommended for publication by Associate Editor H.-J. Kim and Editor L. Moench upon evaluation of the reviewers' comments. This work was supported in part by the Science and Technology Project of State Gird Corporation of China under Grant 5400-202356678A-3-3-JC and in part by the National Natural Science Foundation of China under Grant 62403004, Grant 62203001, Grant 62303009, and Grant 62236002. *(Corresponding author: Chaoxu Mu.)*

Xiasheng Shi and Changyin Sun are with the Key Laboratory of Safety Artificial Intelligence of Anhui Province, the Engineering Research Center of Autonomous Unmanned System Technology, Ministry of Education, and the School of Artificial Intelligence, Anhui University, Hefei 230039, China (e-mail: shixiasheng@zju.edu.cn; cysun@seu.edu.cn).

Chaoxu Mu is with the Key Laboratory of Safety Artificial Intelligence of Anhui Province, Anhui University, Hefei 230039, China, and also with the School of Electrical and Information Engineering, Tianjin University, Tianjin 300072, China (e-mail: cxmu@tju.edu.cn).

Digital Object Identifier 10.1109/TASE.2024.3487214

method was constructed in [14]. However, the continuous-time methods are not easy to implement for the DSP-based controller chip. The reason is that it is not easy to select the proper sampling period for the discretization operation [15]. With this motivation, a discrete-time push-sum-based distributed gradient approach with diminishing step sizes was offered for the distributed EDP over the delayed dynamic networks [16]. This method was further expanded to the general distributed EDP with the assistance of cooperative reinforcement learning [17]. In contrast to the decreasing step size, the incremental cost consensus-based method with fixed control coefficient, as proposed in [18], achieved the global optimal solution by means of a center agent collecting the global mismatch. To eliminate the global information requirement for the center agent, a consensus scheme was developed in [19] to guarantee the power mismatch among agents. It then provided a proportional-integral controller to calculate the output power of a distributed generator. However, the developed method in [19] could not achieve the theoretically optimal solution. To overcome this drawback, a multi-stage distributed bisection algorithm was designed in [20] using a consensus-like iterative approach. Specifically, the scaled power demand was guaranteed in the first stage, and the optimal output power was guaranteed by a centralized min-max operator in the second stage. To simplify the algorithm structure, a novel surplus-based scheme was introduced in [21] to design the economic dispatch algorithm with fixed control parameters, where the surplus variable was established to track the global power balance constraint. In contrast to the surplus-based scheme in [21], an innovative distributed economic dispatch algorithm was proposed through the alternating direction method of multiplier (ADMM) approach for non-quadratic economic dispatch problems [22]. Unlike the above-mentioned continuous communication among agents, a dynamic event-triggered communication mechanism was propounded in [23] to further reduce its communication burden. It is crucial to note that the transmitted information with infinite precision is needed in the aforementioned results for algorithm update and iteration. However, in practice, the communication channel shall be subject to finite bandwidth for the discrete operating system. Thus, it is urgent to research the communication-efficient distributed optimization method for EDPs.

To address this problem, the quantized communication mechanism has been widely deployed in distributed optimization [24], where the information was transformed into a finite discrete group before broadcasting to its neighbors. Plenty of distributed quantized optimization methods have been created for unconstrained convex optimization in recent years, where all agents enjoy the same decision variable. For instance, the innovation compression for gradient tracking methods in [25], and the quantized proportional-integral based method in [26]. However, the local and coupled constraints in EDPs increase the difficulty of its algorithm design and convergence analysis. On this front, a distributed quantized economic dispatch algorithm was developed by converting an analog signal into integers [27], where the quantization error and solution error can be arbitrarily small using proper residue class. To eliminate the quantization error, a dynamic quantization scheme for the quadratic EDP was researched in [28]. It should be stressed that the aforementioned quantized optimization algorithms could only address the quadratic cost function, which cannot be directly implemented in the non-quadratic case of wind turbines in smart grids. Furthermore, the two existing quantization algorithms only achieve the suboptimal results of the EDPs. Therefore, the challenge of tackling the quantized EDP is how to remove the quantization communication error and the accumulated communication error. The above discussions motivate us to study this topic further.

Therefore, we intend to address distributed EDP with non-quadratic cost function under limited communicated bandwidth in this study. We design a quantized distributed optimization approach with a dynamic quantization rule in terms of gradient tracking technology, where an innovative surplus variable is created to prevent the accumulation of quantization errors. In addition, we incorporate a heavy-ball momentum to expedite the convergence process. The contributions include:

- Compared with the distributed EDP with quadratic cost function in [10], [18], [19], [21], [27], and [28], the non-quadratic convex cost function is researched in this study. Although this issue is also considered in [16], [20], [22], [23], [29], [31], [32], and [33], the exact information is required to achieve its optimal solution. The EDP with limited communication bandwidth considered here is more intricate and pragmatic.
- To address the problem of limited communication bandwidth, we propose a robust push-pull-based quantized distributed economic dispatch approach over a directed graph, where the uniform quantizer with finite quantization level is constructed. In addition, we use the contraction theory to provide the convergence domain for the step size and the linear convergence rate for the developed method.

Organization: Section II covers graph theory, problem formulation, and the centralized primal-dual method. Section III develops the quantized economic dispatch approach and its linear convergence rate. We provide the simulation cases and the theoretical findings in Sections IV and V, respectively.

Notations: The real number set with m-dimensions is denoted as $\mathbb{R}^m$. The absolute value, 2-norm, infinite norm, $\mathcal{A}$-norm, and $\mathcal{B}$-norm are respectively described by $|\cdot|$, $\|\cdot\|_2$, $\|\cdot\|_\infty$, $\|\cdot\|_\mathcal{A}$, and $\|\cdot\|_\mathcal{B}$. For instance, the 2-norm is given by $\|x\|_2 = (\sum_{i=1}^n x_i^2)^{\frac{1}{2}}$ with $x = [x_1, x_2, \ldots, x_n]^T \in \mathbb{R}^n$. More definitions can be seen in [25]. The sign function is represented as sign$(\cdot)$. For a matrix $A := [a_{ij}] \in \mathbb{R}^{m\times m}$, $A \preceq 0$ implies that $a_{ij} \leq 0, \forall i, j = 1, 2, \ldots, m$ and the maximum eigenvalue of A is represented by $\rho(A)$.

II. Preliminaries

This section begins with the graph theory for multi-agent systems, and then gives the mathematical form for EDPs. Finally, we introduce the centralized primal-dual methods based on the strongly convex cost function.

A. Graph Theory

In distributed systems, all agents are required to exchange their information over a communication network with neighboring agents. Let $\mathcal{G} = (\mathcal{V}, \mathcal{E})$ to represent the above communication network, which consists of $\mathcal{V}$, a non-empty set of vertices and $\mathcal{E} \subseteq \mathcal{V} \times \mathcal{V}$, a set of edges. An edge $(i, j) \in \mathcal{E}$ implies that agent i can receive data from agent j. In addition, agent j is the in-neighbor of agent i, and agent i is the out-neighbor of agent j. The in- and out-neighbor sets are respectively represented as $\mathcal{N}_i^{\text{in}} = \{j|(i, j) \in \mathcal{E}\} \cup \{i\}$ and $\mathcal{N}_i^{\text{out}} = \{j|(j, i) \in \mathcal{E}\} \cup \{i\}$. The network $\mathcal{G}$ is strongly connected if there exists a closed loop path to connect all agents. For the directed network $\mathcal{G}$, let $\mathcal{B} := [b_{ij}] \in \mathbb{R}^{n\times n}$ and $\mathcal{A} := [a_{ij}] \in \mathbb{R}^{n\times n}$ be two weight matrices so that $\mathcal{A}1_n = 1_n$ and $1_n^T\mathcal{B} = 1_n^T$. For instance, $a_{ij} = \frac{1}{|\mathcal{N}_i^{\text{in}}|}, b_{ij} = \frac{1}{|\mathcal{N}_j^{\text{out}}|}$ if $(i, j) \in \mathcal{E}$ and $a_{ij} = 0, b_{ij} = 0$ otherwise. Besides, let $a_{ii} = \frac{1}{|\mathcal{N}_i^{\text{in}}|}, b_{ii} = \frac{1}{|\mathcal{N}_i^{\text{out}}|}$.

Assumption 1: The directed network $\mathcal{G}$ is strongly connected.

Lemma 1: [29] Let the Assumption 1, $\mathcal{A}_\alpha = I_n+\alpha(\mathcal{A}-I_n)$ and $\mathcal{B}_\beta = I_n + \beta(\mathcal{B} - I_n)$ hold, there exist two matrix norms $\|\cdot\|_\mathcal{A}$ and $\|\cdot\|_\mathcal{B}$ so that $\sigma_\mathcal{A} = \|\mathcal{A}_\alpha - 1_n\pi_\mathcal{A}^T\|_\mathcal{A} < 1$ and $\sigma_\mathcal{B} = \|\mathcal{B}_\beta - \pi_\mathcal{B}1_n^T\|_\mathcal{B} < 1$ where $\pi_\mathcal{A}$ and $\pi_\mathcal{B}$ are respectively the left and right eigenvectors of the matrices $\mathcal{A}$ and $\mathcal{B}$. Moreover, $\pi_\mathcal{A}$ and $\pi_\mathcal{B}$ satisfy that $\pi_\mathcal{A}^T1_n = 1, \pi_\mathcal{A}^T\mathcal{A} = \pi_\mathcal{A}^T$ and $\pi_\mathcal{B}^T1_n = 1, \mathcal{B}\pi_\mathcal{B} = \pi_\mathcal{B}$. Furthermore, there exist positive scalars $\delta_{\mathcal{A}2}, \delta_{\mathcal{B}2}, \delta_{\mathcal{A}\mathcal{B}}$ and $\delta_{\mathcal{B}\mathcal{A}}$ such that $\|\cdot\|_\mathcal{A} \le \delta_{\mathcal{A}\mathcal{B}}\|\cdot\|_\mathcal{B} \le \delta_{\mathcal{B}\mathcal{A}}\|\cdot\|_\mathcal{B}$, $\|\cdot\|_2 \le \|\cdot\|_\mathcal{B} \le \delta_{\mathcal{B}2}\|\cdot\|_2$ and $\|\cdot\|_2 \le \|\cdot\|_\mathcal{A} \le \delta_{\mathcal{A}2}\|\cdot\|_\mathcal{A}$.

B. Problem Formulation

Based on new energy and load forecasting, the distributed EDP aims to allocate the power generation via a distributed way for each generator while minimizing the global objective function, whose structure is described in Fig. 1. Fig. 1 shows that the new power system has a more complex power and energy system structure. The mathematical form is summarized as the following distributed constrained optimization problem:

$$\begin{aligned} &\min_x f(x) = \sum_{i=1}^n f_i(x_i) \\ &\text{s.t.} \sum_{i=1}^n x_i = \sum_{i=1}^n d_i, \, x_i \in [x_i^{\min}, x_i^{\max}], \end{aligned} \tag{1}$$

in which the power generation of ith agent is denoted by $x_i \in \mathbb{R}$. The agent can be a generator or a power plant. In (1), each agent i maintains a private cost function $f_i(x_i) : \mathbb{R} \to \mathbb{R}$ and a private demand power $d_i \in \mathbb{R}$. The cost function $f_i(x_i)$ has different mathematical forms for distinct power generation systems. As an example, $f_i(x_i)$ is a quadratic function in thermal power generation systems [18], and the cost function has exponential terms in wind power generation systems [20]. $x_i^{\max}$ and $x_i^{\min}$ are the specified practical generation constraints. To guarantee the security of information, the local information $f_i(x_i), d_i, x_i^{\min}, x_i^{\max}$ is not allowed to interact among generators.

Assumption 2: For each agent i, the private cost function $f_i(x_i)$ is μ_i-strongly convex and its gradient function $\nabla f_i(x_i)$ is ν_i-Lipschitz continuous. That is, $(x-y)(\nabla f_i(x)-\nabla f_i(y)) \ge \mu_i(x-y)^2$, and $\|\nabla f_i(x) - \nabla f_i(y)\| \le \nu_i\|x-y\|, \forall x, y \in \mathbb{R}$. Additionally, there exists a vector $\tilde{x} \in \mathbb{R}^n$ such that $x_i^{\min} < \tilde{x}_i < x_i^{\max}, \forall i \in \mathcal{V}$ and $\sum_{i=1}^n \tilde{x}_i = \sum_{i=1}^n d_i$.

The above strongly convex property guarantees that the optimal result of problem (1) is unique. The smoothness coefficient ν_i is bigger than the strongly convex coefficient μ_i. Assumption 2 is vital for problem (1) and has been adopted in most existing results [23], [28], [31], under which the linear convergence rate results can be developed. Besides, the quadratic cost function considered in [27] and [28] undoubtedly meets Assumption 2. Finally, the slater's conditions in Assumption 2 ensure that there is no gap between the primal and dual problems to (1).

C. Traditional Lagrange Multiplier Method

To solve the problem (1), the Lagrange multiplied-based primal-dual method has always been used in most existing results, such as the linear algorithm in [31] and the event-triggered algorithm in [23]. From [23] and [31], in view of the Lagrange multiplier λ, we define the dual formula of problem (1) as

$$\max_\lambda q(\lambda) = \sum_{i=1}^n q_i(\lambda), \tag{2}$$

in which $q_i(\lambda) = -f_i^\otimes(\lambda) + \lambda d_i = -\sup_{x_i\in X_i}\{\lambda x_i - f_i(x_i)\} + \lambda d_i$ and $\nabla q_i(\lambda) = -(x_i - d_i)$. In addition, $f_i^\otimes(\lambda) = \sup_{x_i\in X_i}\{\lambda x_i - f_i(x_i)\}$ is the conjugate function of $f_i(x_i)$.

Based on Assumption 2, there must exist at least one optimum Lagrangian multiplier λ^* such that $f(x^*) = q(\lambda^*)$ with optimal solution x^* [31]. In addition, the following Lemma can be developed.

Lemma 2: [32] Considering that Assumption 2 holds, x^* represents the global optimum result of EDP (1) if and only if there exists at least one optimal Lagrangian multiplier λ^* such that

$$\begin{aligned} x_i^* &= \phi_i(\lambda^*) \\ &= \begin{cases} x_i^{\min} & \lambda^* < \nabla f_i(x_i^{\min}) \\ \nabla f_i^{-1}(\lambda^*) & \nabla f_i(x_i^{\min}) \le \lambda^* \le \nabla f_i(x_i^{\max}) \\ x_i^{\max} & \nabla f_i(x_i^{\max}) > \lambda^*, \end{cases} \end{aligned} \tag{3}$$

where $\nabla f_i^{-1}(\cdot)$ denotes the inverse of gradient function $\nabla f_i(\cdot)$. Namely, one has $\nabla f_i(x_i^*) = \lambda^*$ when $x_i^* \in [x_i^{\min}, x_i^{\max}]$.

From Lemma 2, it is vital to obtain the optimum Lagrange multiplier λ^* for solving problem (1).

III. Algorithm Development

This section develops the quantization distributed optimization algorithm based on gradient tracking technology. Afterwards, we establish the linear convergence rate using the matrix contraction method.

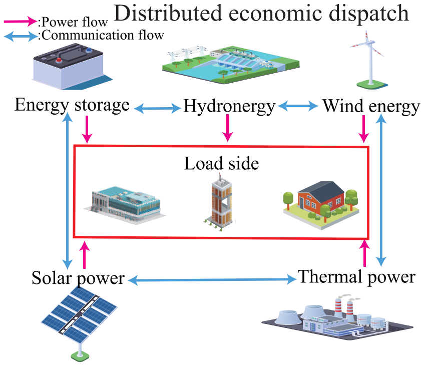

Fig. 1. Structure of distributed economic dispatch in smart grids.

Algorithm 1 Robust Push-Pull-Based Distributed EDP Scheme

Input: input initial variables $x(0), r(0), s(0) \in \mathbb{R}^n$, and control parameter $\beta \in (0,1)$, η in (11), θ in (12)
Output: optimal result x^*
for $\forall i \in \mathcal{V}, t = 1, 2, \ldots$ **do**
  quantizing r_i, s_i according to method (6);
  broadcasting variables $\hat{r}_i(t), \hat{s}_i(t)$ to its neighboring agents;
  receiving variables $\hat{r}_j(t), \hat{s}_j(t)$ from its neighboring agents;
  updating agent state $x_i(t+1), r_i(t+1), s_i(t+1)$ according to method (5);
end

A. Algorithm Design

Before formulating the quantized distributed economic dispatch algorithm, the maximum optimization problem (2) can be reformulated as the following minimum optimization problem.

$$\min_{\lambda} g(\lambda) = \sum_{i=1}^{n} g_i(\lambda) \tag{4}$$

where $g_i(\lambda) = -q_i(\lambda)$ with gradient $\nabla g_i(\lambda) = x_i - d_i$. From (4), all agents share the same decision global decision variable λ. To this end, we allocate one local r_i for each agent i. Subsequently, with the help of consensus protocol in multi-agent systems and gradient tracking technique, we define the following push-pull distributed algorithm:

$$r_i(t+1) = r_i(t) + \alpha \sum_{j=1}^{n} a_{ij}(\hat{r}_j(t) - \hat{r}_i(t)) - \eta(s_i(t) - s_i(t-1)) + \theta(r_i(t) - r_i(t-1)), \tag{5a}$$

$$x_i(t+1) = \min\{\max\{\nabla f_i^{-1}(r_i(t+1)), x_i^{\min}\}, x_i^{\max}\}, \tag{5b}$$

$$s_i(t+1) = (1-\beta)s_i(t) + \beta \sum_{j=1}^{n} b_{ij}\hat{s}_j(t) + x_i(t+1) - d_i, \tag{5c}$$

in which α, β, θ, and η are positive step sizes, and $\hat{r}_j, \hat{s}_j$ are the estimations of the received quantized information. There are two parts in (5). **1) Dual subsystem with (5a) and (5c).** The accumulated communication is removed by designing the robust gradient tracking scheme (5c). In (5c), the surplus variable s_i is proposed to balance the local gradient function $\nabla g_i(r_i)$ such that $\beta(\mathcal{B} - I_n)s^* + x^* - d = 0$ as $t \to \infty$, where each agent pushes the estimated gradient to its neighbors. Since the matrix $\mathcal{B}$ is column stochastic, the equality constraint $1_n^T(x^* - d) = 0$ holds. Thus, the difference $s_i(t+1) - s_i(t)$ is designed to estimate the value of the average dual gradient $\frac{1}{n}\sum_{i=1}^{n}(x_i - d_i)$. Then, based on this estimator and the consensus technique, the variable r_i is proposed in (5a) by means of the descent gradient flow, where the dual variable $\hat{r}_j$ is pulled from its neighbors. In addition, to accelerate the convergence rate of the variable r_i, the heavy-ball momentum $\theta(r_i(t) - r_i(t-1))$ with coefficient θ is adopted in (5a). From (5), the values of variables $r_j(t)$ and $s_j(t)$ from neighboring agents are required to update the decision variable $x_i(t)$, which indicates that our designed algorithm (5) is distributed. Additionally, the dynamic encoding-decoding scheme is introduced to reduce the size of data transmission between neighboring agents. Therefore, the values for variables $r_j(t)$ and $s_j(t)$ should be quantized before sending them to their neighbors. From the definitions of matrix $\mathcal{A}$, the assignment of "pull" weight a_{ij} is straightforward since each agent can easily obtain its in-degree. Similarly, the assignment of "push" is complemented by having the knowledge of their out-degree. Thus, the dual subsystem with (5a) and (5c) is named by a push-pull approach. **2) Primal subsystem with (5b).** After obtaining the dual variable $\lambda_i(t+1)$ in (5a), the decision variable $x_i(t+1)$ is obtained in (5c) based on Lemma 2.

Next, we intend to design the quantization rule for approach (5). Let c_j^r be the internal variable for variable r_j, which is encoded by

$$c_j^r(t) = Q_{K_r}(u_j) = \begin{cases} 0, & -\frac{1}{2} < u_j \le \frac{1}{2} \\ l \cdot \mathrm{sign}(u_j), & \frac{2l-1}{2} < |u_j| \le \frac{2l+1}{2} \\ K_r \cdot \mathrm{sign}(u_j), & |u_j| > \frac{2K_r+1}{2} \end{cases} \tag{6}$$

in which $0 \le l \le K_r$, $u_j = \frac{1}{h(t)}(r_j(t) - \hat{r}_j(t-1))$, $\hat{r}_j(-1) = 0$, and the decaying scaling function $h(t)$ is introduced to eliminate the quantization error. The above quantization rule is bounded by the constant K_r. Then, agent j sends the quantized internal value $c_j^r(t)$ to its neighbors. After receiving the information c_j^r, we need to develop the estimation of $r_j(t)$ by $\hat{r}_j(t) = h(t)c_j^r(t) + \hat{r}_j(t-1)$. It follows from $\|u_j(t)\|_\infty \le K_r + \frac{1}{2}$ that $\|u_j(t) - c_j^r(t)\|_\infty \le \frac{1}{2}$, which means that variable $u_j(t)$ is bounded, and the quantizer is unsaturated. In addition, the variable $s_j(t)$ is quantized in a similar way. The developed method can be summarized in Algorithm 6. Each agent needs to communicate with neighboring agents by $2|N_i|$ times at every iteration and computes $3|N_i| + 12$ times at every iteration.

Remark 1: In [27] and [28], the following gradient tracking method is provided to estimate the global dual gradient *function* $\sum_{i=1}^{n}(x_i - d_i)$.

$$s_i(t+1) = \sum_{j=1}^{n} b_{ij} s_j(t) - (x_i(t+1) - x_i(t)). \quad (7)$$

Then, the surplus variable s_i *instead of the difference variable* $s_i(t) - s_i(t-1)$ *is used to optimize the dual variable* r_i*. In (7), one has the result* $1_n^T s(t+1) = 1_n^T s(t) - 1_n^T x(t+1) + 1_n^T x(t)$*. It yields that* $1_n^T s(t+1) + 1_n^T x(t+1) = 1_n^T s(0) + 1_n^T x(0) = 1_n^T d$*. However, one has the similar result* $1_n^T s(t+1) + 1_n^T x(t+1) = 1_n^T s(t) + 1_n^T x(t) + 1_n^T(\hat{s}(t) - s(t)) = 1_n^T d + \sum_{k=0}^{t} 1_n^T(\hat{s}(k) - s(k))$ *when the quantization communication is introduced. Therefore, the quantization error is accumulated. It is obvious that the surplus variable* s_i *cannot exactly estimate the global dual gradient function. In (5), since* $s(t) - \hat{s}(t) \to 0$ *as* t *goes to infinite, one has the conclusion* $1_n^T s(t+1) - 1_n^T s(t) \to 1_n^T x(t+1) - 1_n^T d$ *as* t *goes to infinite. Thus, the difference variable* $s_i(t+1) - s_i(t)$ *exactly estimate the global dual gradient function* $\sum_{i=1}^{n}(x_i - d_i)$ *when the quantization communication mechanism is applied. Furthermore, compared the initial constraint* $1_n^T s(0) + 1_n^T x(0) = 1_n^T d$ *in [27] and [28], the variable* s *in our developed method is initialization-free. Thus, our proposed method is more robust. Furthermore, the out-degree can be estimated in a distributed way [30].*

Remark 2: To deal with the local capacity constraint, the projection operator in (5b) is introduced via computing the inverse of the gradient function $f_i(\cdot)$*. The computational complexity relies on the computation of inverse function* $\nabla f_i^{-1}(\cdot)$*. Although the limited communication bandwidth is also considered in [27] and [28] where the singular perturbation method is adopted to state its convergence results, the EDP with general cost function instead of the quadratic cost function is considered here. In addition, the surplus* s *in (5) aims to estimate the term* $(\mathcal{B} - I_n)^{-1}(d - x)$ *instead of the term* $x - d$ *in work [32]. Therefore, the quantization errors of the developed algorithm in [27] and [28] are accumulated, and thus, the exact optimal solution cannot be obtained.*

B. Optimality Proof

Before developing the detailed optimality proof, we will show the strongly convex and Lipschitz smooth properties in Lemma 3, the algorithm iterative structure in Lemma 4, and the convergence domain of parameters η and θ in Lemma 5. Then, we show the unsaturation property of the designed quantization scheme in Theorem 1. Finally, we develop the linear convergence performance in Theorem 2.

Lemma 3: [31], [33] Let Assumption 2 hold, the dual convex $g_i(\cdot)$ *is strongly convex with positive constant* $\frac{1}{\nu_i}$ *and Lipschitz smooth with positive constant* $\frac{1}{\mu_i}$*. Besides, let* $\frac{1}{\mu} = \max_i \frac{1}{\mu_i}$ *and* $\frac{1}{\nu} = \min_i \frac{1}{\nu_i}$.

Lemma 3 shows that the strongly convex and smooth property of the dual cost function $g_i(r_i)$ hold, which is related to the primal cost function $f_i(x_i)$. Let $r(t), s(t)$, and $z(t) = s(t) - s(t-1)$ represent their aggregate vectors, then we obtain the subsequent result.

Lemma 4: Let Assumptions 1 and 2 hold. Define $\Psi(t) := [\|r(t) - r(t-1)\|_2, \|\bar{r}(t) - \lambda^*\|_2, \|r(t) - 1_n\bar{r}(t)\|_{\mathcal{A}}, \|z(t) - \pi_{\mathcal{B}}^T \bar{z}(t)\|_{\mathcal{B}}]^T$*, where* $\bar{r}(t) = \pi_{\mathcal{A}}^T r(t)$ *and* $\bar{z}(t) = 1_n^T z(t)$*. Let* $\kappa_1 = \|I_n - 1_n \pi_{\mathcal{A}}^T\|_{\mathcal{A}}, \kappa_2 = \|\pi_{\mathcal{B}}\|_{\mathcal{A}}, \kappa_3 = \|I_n - 1_n \pi_{\mathcal{B}}^T\|_{\mathcal{B}}$, $\kappa_4 = \|\mathcal{A} - I_n\|_2$, $\sigma_r(t) = [\hat{r}_1(t) - r_1(t), \ldots, \hat{r}_n(t) - r_n(t)]^T \in \mathbb{R}^n$*, and* $\epsilon_s(t) = [\epsilon_{s1}(t), \ldots, \epsilon_{sn}(t)]^T \in \mathbb{R}^n$ *with* $\epsilon_{si} = \beta \sum_{j=1}^{n} b_{ij}(\hat{s}_j(t) - s_j(t))$*. If the control parameter* $\eta < \frac{\mu\nu}{(\mu+\nu)\pi_{\mathcal{A}}^T \pi_{\mathcal{B}}}$*, one has*

$$\Psi(t+1) \preceq G\Psi(t) + \varphi(t), \quad (8)$$

in which $G \in \mathbb{R}^{4\times 4}$ *is given by*

$$\begin{aligned}
&G_{11} = \theta, G_{12} = \eta n \frac{1}{\mu}, G_{13} = \alpha\kappa_4 + \eta\sqrt{n}\frac{1}{\mu}, G_{14} = \eta \\
&G_{21} = \theta, G_{22} = (1 - \eta\pi_{\mathcal{A}}^T \pi_{\mathcal{B}} \frac{1}{\nu}), G_{23} = \eta n \pi_{\mathcal{A}}^T \pi_{\mathcal{B}} \frac{1}{\mu}, \\
&G_{24} = \eta, G_{31} = \theta\kappa_1\delta_{\mathcal{A}2}, G_{32} = \eta n \frac{1}{\mu}\kappa_1\kappa_2\delta_{\mathcal{A}2}, \\
&G_{33} = (\sigma_{\mathcal{A}} + \eta\sqrt{n}\kappa_1\kappa_2\delta_{\mathcal{A}2}\frac{1}{\mu}), G_{34} = \eta\kappa_1\delta_{\mathcal{A}\mathcal{B}}, \\
&G_{41} = \theta\kappa_3\delta_{\mathcal{B}2}\frac{1}{\mu}, G_{42} = \eta n \kappa_3\delta_{\mathcal{B}2}\frac{1}{\mu^2}, \\
&G_{43} = \kappa_3\delta_{\mathcal{B}2}(\alpha\kappa_4\frac{1}{\mu} + \eta\sqrt{n}\frac{1}{\mu^2}), G_{44} = \sigma_{\mathcal{B}} + \eta\kappa_3\delta_{\mathcal{B}2}\frac{1}{\mu},
\end{aligned} \quad (9)$$

and $\varphi(t) \in \mathbb{R}^4$ *given by*

$$\begin{aligned}
&\varphi_1(t) = \eta\|1_n^T \epsilon_s(t-1)\|_2 + \alpha\kappa_4\|\sigma_r(t)\|_2, \\
&\varphi_2(t) = \eta\pi_{\mathcal{A}}^T \pi_{\mathcal{B}}\|1_n^T \epsilon_s(t-1)\|_2, \\
&\varphi_3(t) = \eta\kappa_1\kappa_2\delta_{\mathcal{A}2}\|1_n^T \epsilon_s(t-1)\|_2 + \alpha\kappa_4\|\sigma_r(t)\|_{\mathcal{A}}, \\
&\varphi_4(t) = \alpha\kappa_3\kappa_4\delta_{\mathcal{B}2}\frac{1}{\mu}\|\sigma_r(t)\|_2 + \eta\kappa_3\delta_{\mathcal{B}2}\frac{1}{\mu}\|1_n^T \epsilon_s(t-1)\|_2 \\
&\qquad + \kappa_3\|\epsilon_s(t) - \epsilon_s(t-1)\|_{\mathcal{B}}.
\end{aligned} \quad (10)$$

Proof: See Appendix A. □

From (8), we have $\Psi(t) \leq G^t\Psi(0) + \sum_{l=0}^{t-1} G^l \delta(t-1-l)$. If $\rho(G) < 1$ and $\delta(t) \to 0$ as $t \to \infty$, then we can conclude that $\Psi(t) \to 0$ as $t \to \infty$. The following Lemma 5 claims the result $\rho(G) < 1$.

Lemma 5: Given Assumptions 1 and 2, if the control parameters η *and* θ *satisfy*

$$\eta < \min\{\frac{\mu\nu}{(\mu+\nu)\pi_{\mathcal{A}}^T\pi_{\mathcal{B}}}, \frac{(1-\sigma_{\mathcal{A}})\mu}{2\sqrt{n}\kappa_1\kappa_2\delta_{\mathcal{A}2}}, \frac{(1-\sigma_{\mathcal{B}})\mu}{2\delta_{\mathcal{B}2}\kappa_3}, \frac{2\Gamma_{\theta,3}}{\Gamma_{\theta,2} + \sqrt{\Gamma_{\theta,2}^2 + 4\Gamma_{\theta,1}\Gamma_{\theta,3}}}\}, \quad (11)$$

and

$$\theta < \min\{\frac{\Gamma_2}{\Gamma_2 - \hat{\Gamma}_2}, \frac{\Gamma_3}{\Gamma_3 - \hat{\Gamma}_3}\}, \quad (12)$$

where the constants $\Gamma_i, \hat{\Gamma}_i$*, and* $\Gamma_{\theta,i}$ *are defined in (37), (40), and (41). Then, we have the result* $\rho(G) < 1$.

Proof: See Appendix B. □

Theorem 1: Given Assumptions 1 and 2. Let $h(t) = C\xi^t$*, where* $\xi \in (\hat{\rho}, 1)$ *with* $\hat{\rho} = \rho(G) + \varpi < 1$ *for arbitrarily small constant* $\varpi > 0$*, and* C *and* τ *are two positive constants. The step size* η *is given by (11) and* θ *given by (12). Then,* *the quantizers keeps unsaturated providing that K_s and K_r satisfies the subsequent inequalities*:

$$K_r \geq \max\{\frac{v_1}{C}-\frac{1}{2}, \frac{\tau\|\Psi(0)\|_2}{C\xi}\hat{\Upsilon}+\frac{1}{2\xi}-\frac{1}{2}\},$$
$$K_s \geq \max\{\frac{v_2}{C}-\frac{1}{2}, \frac{\sqrt{3}\varepsilon\tau\|\Psi(0)\|_2}{C\xi}\hat{\Upsilon}+\frac{n\beta+1}{2\xi}-\frac{1}{2}\}, \quad (13)$$

where $v_1 = \max_i \|r_i(0)\|_\infty$, $v_2 = \max_i \|s_i(0)\|_\infty$, $\varepsilon = \max\{1, \sqrt{n}\frac{1}{\mu}, n\frac{1}{\mu}\}$, *and* $\hat{\Upsilon} = 1 + \frac{\tilde{\varsigma}\hat{\rho}}{\xi(\xi-\hat{\rho})\|\Psi(0)\|_2} + \frac{\tilde{\varsigma}}{\xi\tau\|\Psi(0)\|_2}$ *with the constant* $\tilde{\varsigma}$ *defined as (18)*.

Proof: We will prove the above conclusion in the following two steps. Step 1: Let's develop the upper bound for $\|y_i(t)-\hat{y}_i(t-1)\|_\infty$ and $\|s_i(t)-\hat{s}_i(t-1)\|_\infty$. Step 2: Determine the lower bound for K_y and K_s by the mathematical induction.

Step 1: Let $e_{ri}(t) = Q_{K_r}(\frac{r_i(t)-\hat{r}_i(t-1)}{h(t)}) - \frac{r_i(t)-\hat{r}_i(t-1)}{h(t)}$ and $e_{si}(t) = Q_{K_s}(\frac{s_i(t)-\hat{s}_i(t-1)}{h(t)}) - \frac{s_i(t)-\hat{s}_i(t-1)}{h(t)}$. Together with the definition of $\hat{r}_j(t)$, it yields that $\hat{r}_j(t) = r_j(t) + h(t)e_{ri}(t)$. Then, we have

$$\begin{aligned}&\|r_i(t)-\hat{r}_i(t-1)\|_\infty\\ &\quad\leq \|r_i(t)-r_i(t-1)\|_\infty + h(t-1)\|e_{ri}(t-1)\|_\infty\\ &\quad\leq \|\Psi_1(t)\| + h(t-1)\max_i\|e_{ri}(t-1)\|_\infty\\ &\quad\leq \|\Psi(t)\| + h(t-1)\max_i\|e_{ri}(t-1)\|_\infty. \end{aligned}\quad (14)$$

Similarly, we have

$$\begin{aligned}&\|s_i(t)-\hat{s}_i(t-1)\|_\infty\\ &\leq \|s_i(t)-s_i(t-1)+s_i(t-1)-\hat{s}_i(t-1)\|_\infty\\ &\leq \|z_i(t)-\pi_{\mathcal{B}}\bar{z}(t)+\pi_{\mathcal{B}}\bar{z}(t)\|_\infty\\ &\quad + h(t-1)\|e_{si}(t-1)\|_\infty\\ &\leq \|\Psi_4(t)\|_2 + \|\bar{z}(t)\|_\infty + h(t-1)\|e_{si}(t-1)\|_\infty\\ &\leq \sqrt{3}\varphi\|\Psi(t)\|_2 + (\beta n+1)h(t-1)\max_i\|e_{si}(t-1)\|_\infty. \end{aligned}\quad (15)$$

In the above third inequality, the result $\|\pi_{\mathcal{B}}\|_\infty \leq 1$ is used. $\|1_n^T\epsilon_s(t-1)\|_\infty \leq n\beta\|\sigma_s(t-1)\|_\infty = n\beta h(t-1)\max_i\|e_{si}(t-1)\|_\infty$ are utilized in the fourth inequality. From (14) and (15), it can be concluded that if the quantizer keeps unsaturated all the time, then $r(t)-\hat{r}(t-1)$ and $s(t)-\hat{s}(t-1)$ approach to zero with convergence speed $O(\xi^{t-1})$. In addition, from (14) and (15), if the scaling function $h(t)$ is not used, i.e., the method shown in [27], then the quantization error will always exist.

Step 2: We first demonstrate the unsaturation by the following time-varying quantization levels

$$\begin{aligned}&K_r(0) \geq \frac{v_1}{C}-\frac{1}{2}, K_s(0) \geq \frac{v_2}{C}-\frac{1}{2},\\ &K_r(t) \geq \frac{\tau\|\Psi(0)\|_2}{C\xi}\Upsilon(t)+\frac{1}{2\xi}-\frac{1}{2}, t\geq 1,\\ &K_s(t) \geq \frac{\sqrt{3}\varphi\tau\|\Psi(0)\|_2}{C\xi}\Upsilon(t)+\frac{n\beta+1}{2\xi}-\frac{1}{2}, t\geq 1, \end{aligned}\quad (16)$$

where $\Upsilon(t) = \left(\frac{\hat{\rho}}{\xi}\right)^t + \frac{\tilde{\varsigma}}{\xi\|\Psi(0)\|_2}\sum_{l=0}^{t-1}\left(\frac{\hat{\rho}}{\xi}\right)^{t-1-l} + \frac{\tilde{\varsigma}}{\tau\xi\|\Psi(0)\|_2}$.

Considering the case $t = 0$, we have $\frac{\|r_i(t)-\hat{r}_i(t-1)\|_\infty}{h(t)} \leq \frac{\|\lambda_i(0)\|_\infty}{C} \leq K_r(0)+\frac{1}{2}$ and $\frac{\|s_i(t)-\hat{s}_i(t-1)\|_\infty}{h(t)} \leq \frac{\|s_i(0)\|_\infty}{C} \leq K_s(0)+\frac{1}{2}$, which implies the quantizers are unsaturated for $t = 0$. Thus, $\max_i\|e_{ri}(0)\|_\infty \leq \frac{1}{2}$ and $\max_i\|e_{si}(0)\|_\infty \leq \frac{1}{2}$ both hold.

Now, considering case $t = 1$. From (14), we have $\frac{\|r_i(1)-\hat{r}_i(0)\|_\infty}{h(1)} \leq \frac{\tau}{C\xi}\|\Psi(0)\|_2 + \frac{1}{\xi}\|e_{ri}(0)\|_\infty \leq \frac{\tau}{C\xi}\|\Psi(0)\|_2 + \frac{1}{2\xi} \leq K_r(1)+\frac{1}{2}$. Similarly, it can easily be verified that $\frac{\|s_i(1)-\hat{s}_i(0)\|_\infty}{h(1)} \leq K_s(1)+\frac{1}{2}$. Therefore, we have $\max_i\|e_{ri}(t)\|_\infty \leq \frac{1}{2}$ and $\max_i\|e_{si}(t)\|_\infty \leq \frac{1}{2}$ for $t = 0, 1$.

Let the result in Theorem 1 hold for $t = t'$. Now, we prove that it is also true for case $t = t'+1$. Based on (14), one obtains that

$$\begin{aligned}\frac{\|r_i(t'+1)-r_i(t')\|_\infty}{h(t'+1)} &\leq \frac{\|\Psi(t')\|_2}{C\xi^{t'+1}}+\frac{1}{2\xi}\\ &\leq \frac{1}{C\xi^{t'+1}}(\tau\|\Psi(0)\|_2\hat{\rho}^{t'}+\tilde{\varsigma}\sum_{l=0}^{t'-1}\hat{\rho}^{t'-1-l}\xi^l+\tilde{\varsigma}\xi^{t'-1})+\frac{1}{2\xi}\\ &\leq K_r(t'+1)+\frac{1}{2}, \end{aligned}\quad (17)$$

where $\tilde{\varsigma} = \|\bar{\varsigma}\in\mathbb{R}^4\|_2$ is defined as

$$\begin{aligned}&\bar{\varsigma}_1 = \frac{1}{2\xi}n\eta\beta C+\frac{1}{2}\alpha\kappa_4\sqrt{n}C, \bar{\varsigma}_2 = \frac{1}{2\xi}n\eta\pi_{\mathcal{A}}^T\pi_{\mathcal{B}}\beta C,\\ &\bar{\varsigma}_3 = \frac{1}{2\xi}n\eta\kappa_1\kappa_2\delta_{\mathcal{A}2}\beta C+\frac{1}{2}\alpha\kappa_4\sqrt{n}C,\\ &\bar{\varsigma}_4 = \frac{1}{2\xi}n\kappa_3\delta_{\mathcal{B}2}\beta C(1+\xi+\eta\frac{1}{\mu})+\frac{1}{2\mu}n\alpha\kappa_3\kappa_4\delta_{\mathcal{B}2}\beta C. \end{aligned}\quad (18)$$

In (18), the results $\|e_{ri}(l)\|_\infty \leq \frac{1}{2}$ and $\|e_{si}(l)\|_\infty \leq \frac{1}{2}, \forall l \leq t'$, are used. From (17), it can be claimed that the quantizer in (5) is unsaturated by the mathematical induction. We can obtain the result for $\frac{\|s_i(t'+1)-s_i(t')\|_\infty}{h(t'+1)} \leq K_s(t'+1)+\frac{1}{2}$ in a similar way. Furthermore, it is obvious that $\Upsilon(t)$ is smaller than $\hat{\Upsilon} = 1+\frac{\tilde{\varsigma}}{\xi\tau|\Psi(0)\|_2}+\frac{\tilde{\varsigma}\hat{\rho}}{\xi(\xi-\hat{\rho})\|\Psi(0)\|_2}$. Thus, the results in Theorem 1 are obtained. □

Theorem 1 shows that the saturation case in (6) can be avoided by selecting sufficiently large constants K_s and K_r. However, more significant values for K_s and K_r result in a higher quantization level. Therefore, one can set a bigger constant C in $h(t) = C\xi^t$ for a low quantization level.

Theorem 2: Let Assumptions 1, 2, and the conditions in (11), (12), and (13) hold. The state generated by (5) with quantization rule (6) achieves x^* *with the convergence speed* $O(\xi^t)$. *Namely,* $\|x_i(t)-x_i^*\|_2 = O(\xi^t), \forall i \in \mathcal{V}$.

Proof: Reconsidering (8) and $\|G(t)\|_2 \leq \tau\hat{\rho}^t$, we have

$$\begin{aligned}\|\Psi(t)\|_2 &\leq \|G^t\|_2\|\Psi(0)\|_2+\tilde{\varsigma}\sum_{l=0}^{t-1}\|G^{t-1-l}\|_2\xi^l\\ &\leq \tau\|\Psi(0)\|_2\hat{\rho}^t+\tilde{\varsigma}\sum_{l=0}^{t-1}\hat{\rho}^{t-1-l}\xi^l\\ &\leq \tau(\|\Psi(0)\|_2\hat{\rho}^t+\frac{\tilde{\varsigma}}{\xi-\hat{\rho}}\xi^t)\\ &\leq \tau(\|\Psi(0)\|_2+\frac{\tilde{\varsigma}}{\xi-\hat{\rho}})\xi^t, \end{aligned}\quad (19)$$

which yields that $\|\Psi(t)\|_2$ achieves zero with rate of $O(\xi^t)$. Thus, we have $\|r_i(t)-\lambda^*\|_2 = O(\xi^t)$. Then, based on algorithm (5), we have the result $\|x_i(t)-x_i^*\|_2 = O(\xi^t)$. □

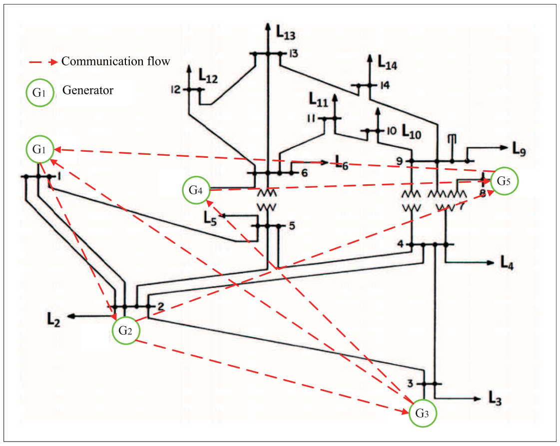

Fig. 2. IEEE 14-BUS system.

IV. Simulation

We present two examples to demonstrate the developed theoretical findings. The quadratic EDP in the first example aims to indicate our created theoretical findings and compares the convergence performance with existing results. The second case aims to test our created methods for dynamic EDPs with non-quadratic cost functions.

Example 1: As shown in Fig. 2, we adopt the data derived from the five generators-based IEEE 14-BUS system [31], where the communication weight is specified as $a_{11} = a_{13} = a_{15} = \frac{1}{3}, a_{12} = a_{22} = \frac{1}{3}, a_{32} = a_{33} = \frac{1}{2}, a_{43} = a_{44} = \frac{1}{2}, a_{52} = a_{54} = a_{55} = \frac{1}{3}$ and $b_{11} = b_{21} = \frac{1}{2}, b_{13} = b_{23} = b_{33} = \frac{1}{3}, b_{15} = b_{55} = \frac{1}{2}, b_{22} = b_{32} = b_{52} = \frac{1}{3}, b_{44} = b_{54} = \frac{1}{2}$. The individual quadratic cost function is defined as $f_i(x_i) = \gamma_{i1}x_i^2 + \gamma_{i2}x_i + \gamma_{i,3}, \forall i \in \mathcal{V}$, with $\gamma_1 = [0.04, 0.03, 0.035, 0.03, 0.04]^T \in \mathbb{R}^5$ and $\gamma_2 = [2, 3, 4, 4, 2.5]^T \in \mathbb{R}^5$. The local demand output is $d = [60, 80, 80, 80, 80]^T \in \mathbb{R}^5$, and the local limitations are $x^{\min} = [0, 0, 0, 0, 0]^T \in \mathbb{R}^5$ and $x^{\max} = [80, 90, 70, 70, 80]^T \in \mathbb{R}^5$. The control parameters or step sizes are set as $\theta = 0.5, \beta = 0.5, \alpha = 0.5, \eta = 0.003, K_r = K_s = 500, C = 100$, and $\xi = 0.95$. Let the initial values of x, r, and s be zero. We depict the simulation curves of variables x_i and $r_i, \forall i \in \mathcal{V}$, in Figs. 3 and 4. The optimal result $x^* = [80, 90, 64.67, 70, 75.33]^T \in \mathbb{R}^5$ shown in Fig. 3 is the same with [31], which indicates that our developed methods can address the EDP accompanied by limited communication bandwidth. Fig. 4 implies that all the local Lagrange multiplier $r_i, \forall i \in \mathcal{V}$, achieve consensus with optimal solution $\lambda^* = 8.52$. Then, we compare our proposed algorithms with existing quantized economic dispatch algorithms in [27] and [28] under the same initial values and control parameters. As shown in Theorem 1, the quantization error in [27] always exists. Although the decreasing scaling function $h(t)$ has also used in [28], Like showing in Remark 2, the surplus variable in [27] and [28] accumulates the quantization error $\sigma_s(t)$ by $\sum_{l=0}^{t} \sigma_s(l)$. The exact optimal output can be obtained if we have $\sum_{l=0}^{t} \sigma_s(l)$. However, the quantization rule in [27] and [28] cannot meet the above condition. Thus, the total equality constraint in problem (1) is not satisfied. Fig. 5 reveals that the existing algorithms in [27] and [28] cannot approach the exact result, instead converging to a suboptimal result. Therefore, our designed method performs better than the existing quantized methods when addressing the EDP with limited data communication.

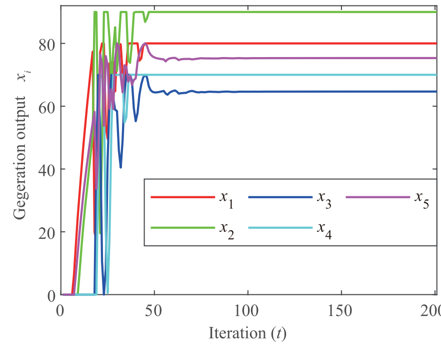

Fig. 3. Simulation results for $x_i, \forall i \in \mathcal{V}$, in Example 1.

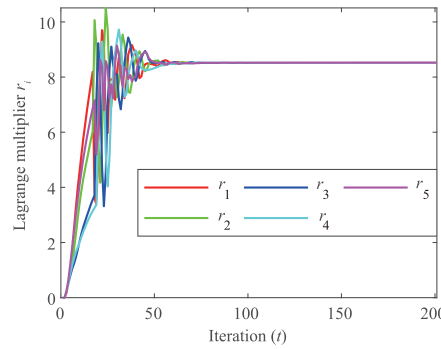

Fig. 4. Simulation results for $r_i, \forall i \in \mathcal{V}$, in Example 1.

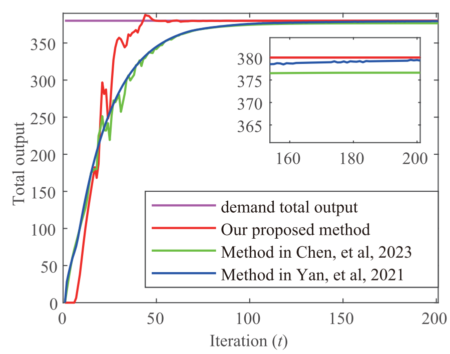

Fig. 5. The comparison for our proposed method and existing methods in Example 1.

Example 2: The simulation material considered here is similar to Example 1, with the exception of the cost function of generator 1 [20], i.e., $f_1(x_1) = \frac{(x_1+25)^2}{25} + 50\exp(\frac{x_1+40}{100})$ under the same control parameters in Example 1. The optimal outputs are shown in Fig. 6. The optimal output $x^* = [69.96, 90, 70, 70, 80]^T \in \mathbb{R}^5$ with optimal Lagrange multiplier $\lambda^* = 9.102$ is achieved, which indicates that our proposed method is valid for the non-quadratic economic dispatch problem. From (5a), we add a momentum $\theta(r_i(t) - r_i(t-1))$ to accelerate the converge speed. Due to the consensus update direction of the agent's state during the algorithm's initial iteration, the current iteration direction is the same as the previous one. Thus, the added heavy-ball momentum accelerates the convergence process. In the later

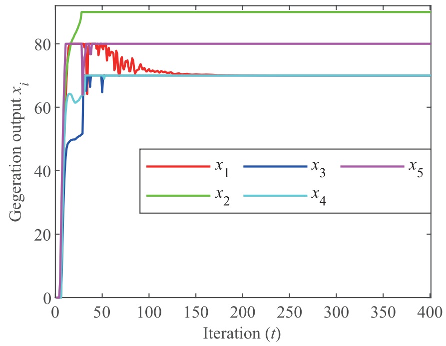

Fig. 6. Simulation results for $x_i, \forall i \in \mathcal{V}$, of static EDP in Example 2.

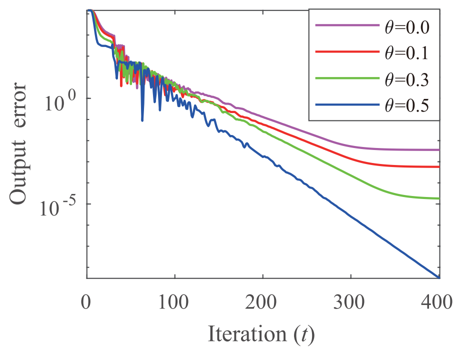

Fig. 7. Simulation results for $e^*(t)$ with different θ in Example 2.

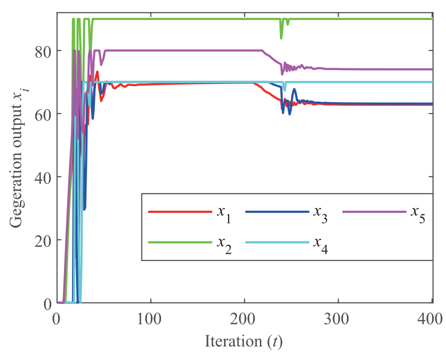

Fig. 8. Simulation results for $x_i, \forall i \in \mathcal{V}$, of dynamic EDP in Example 2.

stage of algorithm iteration, the above two directions are inconsistent. Therefore, the momentum term decreases the convergence process and reduces the oscillation phenomenon of the algorithm at the stable point. Next, we verify the above result shown in Fig. 7 by setting different values for θ, where the output error is defined as $e^*(t) = \frac{1}{2}\sum_{i=1}^{n}\|x_i(t) - x^*\|^2$. Fig. 7 reveals that bigger θ leads to a faster convergence rate, in which $\theta = 0$ indicates the existing algorithm without momentum. Finally, we focus on the time-varying economic dispatch problems. Let $d_1 = 60, t \in [0, 200]$ and $d_1 = 40, t \in [201, 400]$, then Figs. 8 and 9 depict the simulation trajectories of variables x_i and r_i, respectively. The values of $h(t)$ and $s(t)$ in [27] and [28] need to be re-initialized. On the contrary, our proposed method only needs to restart the quantization rule $h(t)$. Hence, it can be concluded that our designed quantized distributed optimization can effectively solve the EDP with limited data communication.

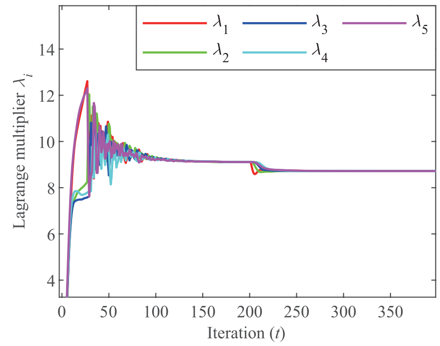

Fig. 9. Simulation results for $r_i, \forall i \in \mathcal{V}$, in Example 2.

V. Conclusion

This study researches distributed EDPs over a digraph with limited data communication by proposing a quantization distributed optimization algorithm, where a dynamic quantization rule is introduced. A robust gradient tracking approach is developed to avoid the accumulation of quantization errors. Besides, the developed method is initialization-free and can be implemented in the dynamic EDPs. Furthermore, a heavy-ball momentum is introduced to accelerate the convergence performance. In the future, we will focus on the event-triggered distributed EDP to reduce the communication burden further.

Appendix

A. Proof of Lemma 4

Proof: Let $k(t) = 1_n^T\nabla g(r(t))$ and $\bar{k}(t) = 1_n^T\nabla g(1_n\bar{r}(t))$. We have $\|k(t)-\bar{k}(t)\|_2 \le \sqrt{n}\frac{1}{\mu}\|r(t)-1_n\bar{r}(t)\|$ by the Lipschitz property of the dual function $g(r)$, $\|\bar{z}(t) - k(t)\| \le \|1_n^T\epsilon_s(t-1)\|_2$ with $\epsilon_{si} = \beta\sum_{j=1}^{n} b_{ij}\sigma_{sj}(t) = \beta\sum_{j=1}^{n} b_{ij}(\hat{s}_j(t) - s_j(t))$, and $\|\bar{g}(t)\|_2 \le n\frac{1}{\mu}\|\bar{r}(t) - \lambda^*\|_2$ by the optimality of $\nabla g(\lambda^*) = 0$. Then, if $\eta \le \frac{\mu\nu}{(\mu+\nu)\pi_{\mathcal{A}}^T\pi_{\mathcal{B}}}$, one has $\|\bar{r}(t)-\eta\pi_{\mathcal{A}}^T\pi_{\mathcal{B}}\bar{k}(t)-\lambda^*\|_2 \le (1-\eta\frac{1}{\nu}\pi_{\mathcal{A}}^T\pi_{\mathcal{B}})\|\bar{r}(t) - \lambda^*\|_2$ by Lemma 1. Now, we begin to limit the term $\Psi(t)$.

First, we begin to bound the average term $\|\bar{z}(t)\|_2$. From (5c), we have

$$\begin{aligned} z(t+1) = {} & \mathcal{B}_\beta z(t) + (\nabla g(r(t+1)) + \epsilon_s(t)) \\ & - (\nabla g(r(t)) + \epsilon_s(t-1)). \end{aligned} \tag{20}$$

Then, in terms of the mathematical induction for (20), it yields that $\bar{z}(t+1) = 1_n^T(\nabla g(r(t+1)) + \epsilon_s(t))$. Therefore, we have

$$\begin{aligned} \|\bar{z}(t)\|_2 & \le \|\bar{z}(t)-k(t)\|_2+\|k(t)-\bar{k}(t)\|_2+\|\bar{k}(t)\|_2 \\ & \le \|1_n^T\epsilon_s(t-1)\|_2+\sqrt{n}\frac{1}{\mu}\|r(t)-1_n\bar{r}(t)\|_{\mathcal{A}} \\ & \quad + n\frac{1}{\mu}\|\bar{r}(t) - \lambda^*\|_2. \end{aligned} \tag{21}$$

Now, from (5a), we have

$$\begin{aligned} & r(t+1) - r(t) \\ & \quad = \alpha(\mathcal{A} - I_n)\sigma_r(t) - \eta z(t) + \alpha(\mathcal{A} - I_n)r(t) \\ & \qquad + \theta(r(t) - r(t-1)) \\ & \quad = \alpha(\mathcal{A} - I_n)\sigma_r(t) - \eta z(t) + \theta(r(t) - r(t-1)) \\ & \qquad + \alpha(\mathcal{A} - I_n)(r(t) - 1_n\bar{r}(t)), \end{aligned} \tag{22}$$

in which the result $(\mathcal{A}-I_n)1_n = 0$ is considered in the second equality. Therefore, by substituting (21) into (22), we obtain

$$\begin{aligned}\Psi_1(t+1) \le & \alpha\kappa_4\|\sigma_r(t)\|_2 + \eta\|\bar{z}(t)\|_2 \\ & + \theta\Psi_1(t) + \alpha\kappa_4\Psi_3(t) + \eta\Psi_4(t) \\ \le & \eta\|1_n^T\epsilon_s(t-1)\|_2 + \alpha\kappa_4\|\sigma_r(t)\|_2 \\ & + \theta\Psi_1(t) + \eta n\frac{1}{\mu}\Psi_2(t) + \eta\Psi_4(t) \\ & + (\alpha\kappa_4 + \eta\sqrt{n}\frac{1}{\mu})\Psi_3(t), \end{aligned} \tag{23}$$

where $\kappa_4 = \|\mathcal{A}-I_n\|_2$, and the results $\|\pi_{\mathcal{B}}^T\|_2 \le 1$ and $\|1_n\|_2 = 1$ have been used.

Second, it follows from (5a) that

$$\begin{aligned}\bar{r}(t+1) = & \bar{r}(t) - \eta\pi_{\mathcal{A}}^T z(t) - \theta\pi_{\mathcal{A}}^T(r(t) - r(t-1)) \\ = & \bar{r}(t) - \eta\pi_{\mathcal{A}}^T\pi_{\mathcal{B}}\bar{z}(t) - \eta\pi_{\mathcal{A}}^T(z(t) - \pi_{\mathcal{B}}\bar{z}(t)) \\ = & \bar{r}(t) - \eta\pi_{\mathcal{A}}^T\pi_{\mathcal{B}}\bar{k}(t) - \eta\pi_{\mathcal{A}}^T\pi_{\mathcal{B}}(\bar{z}(t) - k(t)) \\ & - \eta\pi_{\mathcal{A}}^T\pi_{\mathcal{B}}(k(t) - \bar{k}(t)) - \eta\pi_{\mathcal{A}}^T(z(t) - \pi_{\mathcal{B}}\bar{z}(t)) \\ & - \theta\pi_{\mathcal{A}}^T(r(t) - r(t-1)) \\ = & \bar{r}(t) - \eta\pi_{\mathcal{A}}^T\pi_{\mathcal{B}}\bar{k}(t) - \eta\pi_{\mathcal{A}}^T\pi_{\mathcal{B}}1_n^T\epsilon_s(t-1) \\ & - \eta\pi_{\mathcal{A}}^T\pi_{\mathcal{B}}(k(t) - \bar{k}(t)) - \eta\pi_{\mathcal{A}}^T(z(t) - \pi_{\mathcal{B}}\bar{z}(t)) \\ & - \theta\pi_{\mathcal{A}}^T(r(t) - r(t-1)). \end{aligned} \tag{24}$$

Then, we have

$$\begin{aligned}\Psi_2(t+1) \le & (1 - \eta\pi_{\mathcal{A}}^T\pi_{\mathcal{B}}\frac{1}{\nu})\Psi_2(t) \\ & + \eta\pi_{\mathcal{A}}^T\pi_{\mathcal{B}}\|k(t) - \bar{k}(t)\|_2 + \eta\Psi_4(t) \\ & + \theta\Psi_1(t) + \eta\pi_{\mathcal{A}}^T\pi_{\mathcal{B}}\|1_n^T\epsilon_s(t-1)\|_2 \\ \le & \theta\Psi_1(t) + (1 - \eta\pi_{\mathcal{A}}^T\pi_{\mathcal{B}}\frac{1}{\nu})\Psi_2(t) \\ & + \sqrt{n}\eta\pi_{\mathcal{A}}^T\pi_{\mathcal{B}}\frac{1}{\mu}\Psi_3(t) + \eta\Psi_4(t) \\ & + \eta\pi_{\mathcal{A}}^T\pi_{\mathcal{B}}\|1_n^T\epsilon_s(t-1)\|_2, \end{aligned} \tag{25}$$

where the fact $\|\pi_{\mathcal{A}}\|_2 \le 1$ has been used in the last inequality.

Third, with the help of results $\mathcal{A}_\alpha 1_n = 1_n$ and $\mathcal{A}_\alpha = (1-\alpha)I_n + \alpha\mathcal{A}$, one has

$$\begin{aligned} & r(t+1) - \bar{r}(t+1) \\ & = \mathcal{A}_\alpha(r(t) - 1_n\bar{r}(t)) - \eta(I_n - 1_n\pi_{\mathcal{A}}^T)z(t) \\ & \quad + \alpha(\mathcal{A}-I_n)\sigma_r(t) + \theta(I_n - 1_n\pi_{\mathcal{A}}^T)(r(t) - r(t-1)) \\ & = (\mathcal{A}_\alpha - 1_n\pi_{\mathcal{A}}^T)(r(t) - 1_n\bar{r}(t)) - \eta(I_n - 1_n\pi_{\mathcal{A}}^T)z(t) \\ & \quad + \alpha(\mathcal{A}-I_n)\sigma_r(t) + \theta(I_n - 1_n\pi_{\mathcal{A}}^T)(r(t) - r(t-1)) \\ & = (\mathcal{A}_\alpha - 1_n\pi_{\mathcal{A}}^T)(r(t) - 1_n\bar{r}(t)) - \eta(I_n - 1_n\pi_{\mathcal{A}}^T)\pi_{\mathcal{B}}\bar{z}(t) \\ & \quad - \eta(I_n - 1_n\pi_{\mathcal{A}}^T)(z(t) - \pi_{\mathcal{B}}\bar{z}(t)) + \alpha(\mathcal{A} - I_n)\sigma_r(t) \\ & \quad + \theta(I_n - 1_n\pi_{\mathcal{A}}^T)(r(t) - r(t-1)), \end{aligned} \tag{26}$$

in which the fact $1_n\pi_{\mathcal{A}}^T(r(t) - 1_n\bar{r}(t)) = 0_n$ has been considered in the second equality. Therefore, one has

$$\begin{aligned}\Psi_3(t+1) \le & \theta\kappa_1\delta_{\mathcal{A}2}\Psi_1(t) + \sigma_{\mathcal{A}}\Psi_3(t) + \eta\kappa_1\delta_{\mathcal{AB}}\Psi_4(t) \\ & + \alpha\kappa_4\|\sigma_r(t)\|_{\mathcal{A}} + \eta\kappa_1\kappa_2\delta_{\mathcal{A}2}\|\bar{z}(t)\|_2, \end{aligned} \tag{27}$$

where $\kappa_1 = \|I_n - 1_n\pi_{\mathcal{A}}^T\|_{\mathcal{A}}$, $\kappa_2 = \|\pi_{\mathcal{B}}\|_{\mathcal{A}}$. By substituting (21) into (27), one claims that

$$\begin{aligned}\Psi_3(t+1) \le & \theta\kappa_1\delta_{\mathcal{A}2}\Psi_1(t) + \eta n\frac{1}{\mu}\kappa_1\kappa_2\delta_{\mathcal{A}2}\Psi_2(t) \\ & + (\sigma_{\mathcal{A}} + \sqrt{n}\frac{1}{\mu}\eta\kappa_1\kappa_2\delta_{\mathcal{A}2})\Psi_3(t) \\ & + \eta\kappa_1\delta_{\mathcal{AB}}\Psi_4(t) \\ & + \alpha\kappa_4\|\sigma_r(t)\|_{\mathcal{A}} + \eta\kappa_1\kappa_2\delta_{\mathcal{A}2}\|\epsilon_s(t-1)\|_2. \end{aligned} \tag{28}$$

Similarly, it can be obtained that

$$\begin{aligned} & z(t+1) - \pi_{\mathcal{B}}\bar{z}(t+1) \\ & = (\mathcal{B}_\beta - \pi_{\mathcal{B}}1_n^T)(z(t) - \pi_{\mathcal{B}}\bar{z}(t)) \\ & \quad + (I_n - \pi_{\mathcal{B}}1_n^T)(\nabla g(r(t+1)) - \nabla g(r(t))) \\ & \quad + (I_n - \pi_{\mathcal{B}}1_n^T)(\epsilon_s(t) - \epsilon_s(t-1)), \end{aligned} \tag{29}$$

where we have used the definition $\mathcal{B}_\beta = (1-\beta)I_n + \beta\mathcal{B}$ and the fact $\pi_{\mathcal{B}}1_n^T\pi_{\mathcal{B}} = \pi_{\mathcal{B}}$. Therefore, one has

$$\begin{aligned}\Psi_4(t) \le & \delta_{\mathcal{B}2}\|I_n - \pi_{\mathcal{B}}1_n^T\|_{\mathcal{B}}\|\nabla g(r(t+1)) - \nabla g(r(t))\|_2 \\ & + \delta_{\mathcal{B}2}\|I_n - \pi_{\mathcal{B}}1_n^T\|_{\mathcal{B}}\|\epsilon_s(t) - \epsilon_s(t-1)\|_{\mathcal{B}} \\ & + \sigma_{\mathcal{B}}\Psi_4(t). \end{aligned} \tag{30}$$

Now, we need to bound $\|\nabla g(r(t+1)) - \nabla g(r(t))\|_2$. By the smoothness of the dual function $g(r)$, we have

$$\begin{aligned} & \|\nabla g(r(t+1)) - \nabla g(r(t))\|_2 \le \frac{1}{\mu}\Psi_1(t+1) \\ & \le \frac{1}{\mu}\eta\|1_n^T\epsilon_s(t-1)\|_2 + \frac{1}{\mu}\alpha\kappa_4\|\sigma_r(t)\|_2 \\ & \quad + \theta\frac{1}{\mu}\Psi_1(t) + \eta n\frac{1}{\mu^2}\Psi_2(t) + \frac{1}{\mu}\eta\Psi_4(t) \\ & \quad + \frac{1}{\mu}(\alpha\kappa_4 + \eta\sqrt{n}\frac{1}{\mu})\Psi_3(t), \end{aligned} \tag{31}$$

where we have used the fact that $\|\pi_{\mathcal{B}}\|_2 \le 1$. Finally, we have

$$\begin{aligned} & \Psi_4(t+1) \\ & \le \delta_{\mathcal{B}2}\kappa_3\frac{1}{\mu}\theta\Psi_1(t) + \delta_{\mathcal{B}2}\kappa_3(\alpha\kappa_4\frac{1}{\mu} + \sqrt{n}\eta\frac{1}{\mu^2})\Psi_3(t) \\ & \quad + \delta_{\mathcal{B}2}\kappa_3 n\eta\frac{1}{\mu^2}\Psi_2(t) + (\sigma_{\mathcal{B}} + \delta_{\mathcal{B}2}\eta\frac{1}{\mu}\kappa_3)\Psi_4(t) \\ & \quad + \delta_{\mathcal{B}2}\alpha\frac{1}{\mu}\kappa_3\kappa_4\|\sigma_r(t)\|_2 + \delta_{\mathcal{B}2}\eta\frac{1}{\mu}\kappa_3\|1_n^T\epsilon_s(t-1)\|_2 \\ & \quad + \delta_{\mathcal{B}2}\kappa_3\|\epsilon_s(t) - \epsilon_s(t-1)\|_{\mathcal{B}}, \end{aligned} \tag{32}$$

where $\kappa_3 = \|I_n - \pi_{\mathcal{B}}1_n^T\|_{\mathcal{B}}$. Therefore, the results in (8) hold. □

B. Proof of Lemma 5

Proof: It can be seen from Lemma 5 in [34] that the following conditions are required to guarantee $\rho(G) < 1$. That is, the matrix G requires that all elements are positive, diagonal elements are less than 1, and the determinant of matrix $I_4 - G$ should be greater than zero. The first three terms in (11) and the result $0 < \theta < 1$ can be obtained by the condition $0 < G_{ii} < 1, i = 1, 2, 3, 4$. Now, let's determine the determinant of $I_4 - G$. Then, we have

$$\det(I_4 - G) = (1-\theta)\omega_1 + \theta\omega_2, \tag{33}$$

where

$$
\begin{aligned}
\omega_1 = {} & \eta\pi_{\mathcal{A}}^T\pi_{\mathcal{B}}\frac{1}{\nu}[1-(\sigma_{\mathcal{A}}+\sqrt{n}\eta\frac{1}{\mu}\kappa_1\kappa_2\delta_{\mathcal{A}2})] \\
& \times[1-(\sigma_{\mathcal{B}}+\eta\frac{1}{\mu}\kappa_3\delta_{\mathcal{B}2})] \\
& -\eta\pi_{\mathcal{A}}^T\pi_{\mathcal{B}}\frac{1}{\nu}(\eta\kappa_1\delta_{\mathcal{A}\mathcal{B}})[\kappa_3(\alpha\kappa_4\frac{1}{\mu}+\sqrt{n}\eta\frac{1}{\mu^2})\delta_{\mathcal{B}2}] \\
& -\sqrt{n}\eta\pi_{\mathcal{A}}^T\pi_{\mathcal{B}}\frac{1}{\mu}(n\eta\frac{1}{\mu}\kappa_1\kappa_2\delta_{\mathcal{A}2})[1-(\sigma_{\mathcal{B}}+\eta\frac{1}{\mu}\kappa_3\delta_{\mathcal{B}2})] \\
& -\sqrt{n}\eta\pi_{\mathcal{A}}^T\pi_{\mathcal{B}}\frac{1}{\mu}(n\eta\frac{1}{\mu}\kappa_3\delta_{\mathcal{B}2})(\eta\kappa_1\delta_{\mathcal{A}\mathcal{B}}) \\
& -\eta(n\eta\frac{1}{\mu}\kappa_1\kappa_2\delta_{\mathcal{A}2})[\kappa_3(\alpha\kappa_4\frac{1}{\mu}+\sqrt{n}\eta\frac{1}{\mu^2})\delta_{\mathcal{B}2}] \\
& -\eta[1-(\sigma_{\mathcal{A}}+\sqrt{n}\eta\frac{1}{\mu}\kappa_1\kappa_2\delta_{\mathcal{A}2})](n\eta\frac{1}{\mu}\kappa_3\delta_{\mathcal{B}2}), \qquad (34)
\end{aligned}
$$

and

$$
\begin{aligned}
\omega_2 = {} & -\eta n\frac{1}{\mu}[1-(\sigma_{\mathcal{A}}+\eta\sqrt{n}\kappa_1\kappa_2\delta_{\mathcal{B}2}\frac{1}{\mu})] \\
& \times[1-(\sigma_{\mathcal{B}}+\eta\kappa_3\delta_{\mathcal{B}2}\frac{1}{\mu})] \\
& +\eta^2 n\kappa_1\kappa_3\delta_{\mathcal{A}\mathcal{B}}\delta_{\mathcal{B}2}(\alpha\kappa_4\frac{1}{\mu^2}+\eta\sqrt{n}\frac{1}{\mu^3}) \\
& +\eta n\kappa_1\kappa_2\delta_{\mathcal{A}2}\frac{1}{\mu}[-(\alpha\kappa_4+\eta\sqrt{n}\frac{1}{\mu}) \\
& \times(1-(\sigma_{\mathcal{B}}+\eta\kappa_3\delta_{\mathcal{B}2}\frac{1}{\mu}))] \\
& -\eta^2 n\kappa_1^2\kappa_2\kappa_3\delta_{\mathcal{A}2}\delta_{\mathcal{B}2}(\alpha\kappa_4\frac{1}{\mu^2}+\eta\sqrt{n}\frac{1}{\mu^3}) \\
& -\eta^2 n\kappa_1\kappa_3\delta_{\mathcal{A}\mathcal{B}}\delta_{\mathcal{B}2}\frac{1}{\mu}(\alpha\kappa_4+\eta\sqrt{n}\frac{1}{\mu}) \\
& -\eta^2 n\kappa_3\delta_{\mathcal{B}2}\frac{1}{\mu}[1-(\sigma_{\mathcal{A}}+\eta\sqrt{n}\kappa_1\kappa_2\delta_{\mathcal{B}2}\frac{1}{\mu})] \\
& -\eta^2 n^{\frac{3}{2}}\kappa_1\pi_{\mathcal{A}}^T\pi_{\mathcal{B}}\delta_{\mathcal{A}2}\frac{1}{\mu^2}[1-(\sigma_{\mathcal{B}}+\eta\kappa_3\delta_{\mathcal{B}2}\frac{1}{\mu})] \\
& -\eta^2 n\kappa_1\kappa_3\delta_{\mathcal{A}2}\delta_{\mathcal{B}2}(\alpha\kappa_4\frac{1}{\mu^2}+\eta\sqrt{n}\frac{1}{\mu^3}) \\
& -\eta\kappa_1\pi_{\mathcal{A}}^T\pi_{\mathcal{B}}\delta_{\mathcal{A}2}\frac{1}{\nu}(\alpha\kappa_4+\eta\sqrt{n}\frac{1}{\mu}) \\
& \times[1-(\sigma_{\mathcal{B}}+\eta\kappa_3\delta_{\mathcal{B}2}\frac{1}{\mu})] \\
& -\eta^2\kappa_1\kappa_3\pi_{\mathcal{A}}^T\pi_{\mathcal{B}}\delta_{\mathcal{A}2}\delta_{\mathcal{B}2}\frac{1}{\nu}(\alpha\kappa_4\frac{1}{\mu}+\eta\sqrt{n}\frac{1}{\mu^2}) \\
& +\eta^2 n\kappa_1\kappa_3\delta_{\mathcal{A}2}\delta_{\mathcal{B}2}\frac{1}{\mu}(\alpha\kappa_4+\eta\sqrt{n}\frac{1}{\mu}) \\
& -\eta^3 n^{\frac{3}{2}}\kappa_1\kappa_3\delta_{\mathcal{A}2}\delta_{\mathcal{B}2}\pi_{\mathcal{A}}^T\pi_{\mathcal{B}}\frac{1}{\mu^2} \\
& -\eta^3 n^{\frac{3}{2}}\kappa_1\kappa_3\delta_{\mathcal{A}\mathcal{B}}\delta_{\mathcal{B}2}\pi_{\mathcal{A}}^T\pi_{\mathcal{B}}\frac{1}{\mu^3} \\
& -\eta^2 n\kappa_3\delta_{\mathcal{B}2}\frac{1}{\mu^2}[1-(\sigma_{\mathcal{A}}+\eta\sqrt{n}\kappa_1\kappa_2\delta_{\mathcal{A}2}\frac{1}{\mu})] \\
& -\eta^2\kappa_1\kappa_3\delta_{\mathcal{A}\mathcal{B}}\delta_{\mathcal{B}2}\pi_{\mathcal{A}}^T\pi_{\mathcal{B}}\frac{1}{\mu\nu}(\alpha\kappa_4+\eta\sqrt{n}\frac{1}{\mu}) \\
& -\eta^2\kappa_3\delta_{\mathcal{B}2}\pi_{\mathcal{A}}^T\pi_{\mathcal{B}}\frac{1}{\mu\nu}[1-(\sigma_{\mathcal{A}}+\eta\sqrt{n}\kappa_1\kappa_2\delta_{\mathcal{B}2}\frac{1}{\mu})] \\
& -\eta^2 n\kappa_1\kappa_2\kappa_3\delta_{\mathcal{A}2}\delta_{\mathcal{B}2}\frac{1}{\mu^2}(\alpha\kappa_4+\eta\sqrt{n}\frac{1}{\mu}) \\
& +\eta^3 n^{\frac{3}{2}}\kappa_1\kappa_2\kappa_3\delta_{\mathcal{A}2}\delta_{\mathcal{B}2}\pi_{\mathcal{A}}^T\pi_{\mathcal{B}}\frac{1}{\mu^3}. \qquad (35)
\end{aligned}
$$

In light of $\eta \le \min\{\frac{(1-\sigma_{\mathcal{A}})\mu}{2\sqrt{n}\kappa_1\kappa_2\delta_{\mathcal{A}2}}, \frac{(1-\sigma_{\mathcal{B}})\mu}{2\delta_{\mathcal{B}2}\kappa_3}\}$, we have $\frac{1-\sigma_{\mathcal{A}}}{2} \le 1-(\sigma_{\mathcal{A}}+\sqrt{n}\eta\frac{1}{\mu}\kappa_1\kappa_2\delta_{\mathcal{A}2}) \le 1-\sigma_{\mathcal{A}}$ and $\frac{1-\sigma_{\mathcal{B}}}{2} \le 1-(\sigma_{\mathcal{B}}+\eta\frac{1}{\mu}\kappa_3\delta_{\mathcal{B}2}) \le 1-\sigma_{\mathcal{B}}$. Therefore, the following result can be obtained.

$$
\begin{aligned}
\omega_1 \ge {} & \eta\{\frac{1}{4}\pi_{\mathcal{A}}^T\pi_{\mathcal{B}}\frac{1}{\nu}(1-\sigma_{\mathcal{A}})(1-\sigma_{\mathcal{B}})-(1-\sigma_{\mathcal{A}})(n\eta\frac{1}{\mu}\kappa_3\delta_{\mathcal{B}2}) \\
& -\pi_{\mathcal{A}}^T\pi_{\mathcal{B}}\frac{1}{\nu}(\eta\kappa_1\delta_{\mathcal{A}\mathcal{B}})[\kappa_3(\alpha\kappa_4\frac{1}{\mu}+\sqrt{n}\eta\frac{1}{\mu^2})\delta_{\mathcal{B}2}] \\
& -\sqrt{n}\pi_{\mathcal{A}}^T\pi_{\mathcal{B}}\frac{1}{\mu}(n\eta\frac{1}{\mu}\kappa_1\kappa_2\delta_{\mathcal{A}2})(1-\sigma_{\mathcal{B}}) \\
& -\sqrt{n}\pi_{\mathcal{A}}^T\pi_{\mathcal{B}}\frac{1}{\mu}(n\eta\frac{1}{\mu}\kappa_3\delta_{\mathcal{B}2})(\eta\kappa_1\delta_{\mathcal{A}\mathcal{B}}) \\
& -(n\eta\frac{1}{\mu}\kappa_1\kappa_2\delta_{\mathcal{A}2})[\kappa_3(\alpha\kappa_4\frac{1}{\mu}+\sqrt{n}\eta\frac{1}{\mu^2})\delta_{\mathcal{B}2}]\} \\
= {} & -\eta(\Gamma_1\eta^2+\Gamma_2\eta-\Gamma_3), \qquad (36)
\end{aligned}
$$

where $\Gamma_i, i=1,2,3$ are given by

$$
\begin{aligned}
\Gamma_1 &= \sqrt{n}\kappa_1\kappa_3\delta_{\mathcal{B}2}\frac{1}{\mu^2}[\delta_{\mathcal{A}\mathcal{B}}\pi_{\mathcal{A}}^T\pi_{\mathcal{B}}(n+\frac{1}{\nu})+n\kappa_2\delta_{\mathcal{A}2}\frac{1}{\mu}], \\
\Gamma_2 &= \kappa_1\frac{1}{\mu}\pi_{\mathcal{A}}^T\pi_{\mathcal{B}}[n^{\frac{3}{2}}\kappa_2\delta_{\mathcal{A}2}\frac{1}{\mu}(1-\sigma_{\mathcal{B}})+\alpha\kappa_3\kappa_4\delta_{\mathcal{A}\mathcal{B}}\delta_{\mathcal{B}2}\frac{1}{\nu}] \\
&\quad +n\kappa_3\frac{1}{\mu}\delta_{\mathcal{B}2}[1-\sigma_{\mathcal{A}}+\alpha\kappa_1\kappa_2\kappa_4\delta_{\mathcal{A}2}\frac{1}{\mu}], \\
\Gamma_3 &= \frac{1}{4\nu}\pi_{\mathcal{A}}^T\pi_{\mathcal{B}}(1-\sigma_{\mathcal{A}})(1-\sigma_{\mathcal{B}}). \qquad (37)
\end{aligned}
$$

Similarly, one has

$$
\begin{aligned}
\omega_2 \ge {} & -\eta n\frac{1}{\mu}(1-(\sigma_{\mathcal{A}})(1-\sigma_{\mathcal{B}}) \\
& +\eta^2 n\alpha\kappa_1\kappa_3\kappa_4\delta_{\mathcal{A}\mathcal{B}}\delta_{\mathcal{B}2}\frac{1}{\mu^2} \\
& -\eta n\kappa_1\kappa_2\delta_{\mathcal{A}2}\frac{1}{\mu}(\alpha\kappa_4+\eta\sqrt{n}\frac{1}{\mu})(1-\sigma_{\mathcal{B}}) \\
& -\eta^2 n\kappa_1\kappa_2\kappa_3\delta_{\mathcal{A}2}\delta_{\mathcal{B}2}\frac{1}{\mu^2}(\alpha\kappa_4+\eta\sqrt{n}\frac{1}{\mu}) \\
& -\eta^2 n\kappa_1\kappa_3\delta_{\mathcal{A}\mathcal{B}}\delta_{\mathcal{B}2}\frac{1}{\mu}(\alpha\kappa_4+\eta\sqrt{n}\frac{1}{\mu}) \\
& -\eta^2 n\kappa_3\delta_{\mathcal{B}2}\frac{1}{\mu}(1-\sigma_{\mathcal{A}}) \\
& -\eta^2 n^{\frac{3}{2}}\kappa_1\pi_{\mathcal{A}}^T\pi_{\mathcal{B}}\delta_{\mathcal{A}2}\frac{1}{\mu^2}(1-\sigma_{\mathcal{B}}) \\
& -\eta^2 n\kappa_1\kappa_3\delta_{\mathcal{A}2}\delta_{\mathcal{B}2}\frac{1}{\mu^2}(\alpha\kappa_4+\eta\sqrt{n}\frac{1}{\mu}) \\
& -\eta\kappa_1\pi_{\mathcal{A}}^T\pi_{\mathcal{B}}\delta_{\mathcal{A}2}\frac{1}{\nu}(\alpha\kappa_4+\eta\sqrt{n}\frac{1}{\mu})(1-\sigma_{\mathcal{B}}) \\
& -\eta^2\kappa_1\kappa_3\pi_{\mathcal{A}}^T\pi_{\mathcal{B}}\delta_{\mathcal{A}2}\delta_{\mathcal{B}2}\frac{1}{\nu}\kappa_4\frac{1}{\mu} \\
& +\eta^2 n\kappa_1\kappa_3\delta_{\mathcal{A}2}\delta_{\mathcal{B}2}\frac{1}{\mu}(\alpha\kappa_4+\eta\sqrt{n}\frac{1}{\mu}) \\
& -\eta^3 n^{\frac{3}{2}}\kappa_1\kappa_3\delta_{\mathcal{A}2}\delta_{\mathcal{B}2}\pi_{\mathcal{A}}^T\pi_{\mathcal{B}}\frac{1}{\mu^2}
\end{aligned}
$$

$$
\begin{aligned}
&- \eta^3 n^{\frac{3}{2}} \kappa_1 \kappa_3 \delta_{\mathcal{AB}} \delta_{\mathcal{B}2} \pi_{\mathcal{A}}^T \pi_{\mathcal{B}} \frac{1}{\mu^3} \\
&- \eta^2 n \kappa_3 \delta_{\mathcal{B}2} \frac{1}{\mu^2} (1 - \sigma_{\mathcal{A}}) \\
&- \eta^2 \kappa_1 \kappa_3 \delta_{\mathcal{AB}} \delta_{\mathcal{B}2} \pi_{\mathcal{A}}^T \pi_{\mathcal{B}} \frac{1}{\mu \nu} (\alpha \kappa_4 + \eta \sqrt{n} \frac{1}{\mu}) \\
&- \eta^2 \kappa_3 \delta_{\mathcal{B}2} \pi_{\mathcal{A}}^T \pi_{\mathcal{B}} \frac{1}{\mu \nu} (1 - \sigma_{\mathcal{A}}) \\
&- \eta^2 n \kappa_1 \kappa_2 \kappa_3 \delta_{\mathcal{A}2} \delta_{\mathcal{B}2} \frac{1}{\mu^2} (\alpha \kappa_4 + \eta \sqrt{n} \frac{1}{\mu}) \\
&+ \eta^3 n^{\frac{3}{2}} \kappa_1 \kappa_2 \kappa_3 \delta_{\mathcal{A}2} \delta_{\mathcal{B}2} \pi_{\mathcal{A}}^T \pi_{\mathcal{B}} \frac{1}{\mu^3},
\end{aligned} \tag{38}
$$

where we have used the result $n^{\frac{3}{2}} \kappa_1 \kappa_3 \delta_{\mathcal{AB}} \delta_{\mathcal{B}2} \frac{1}{\mu^3} \geq n \kappa_1 \kappa_3 \delta_{\mathcal{AB}} \delta_{\mathcal{B}2} \pi_{\mathcal{A}}^T \pi_{\mathcal{B}} \frac{1}{\mu^2 \nu}$ in above deduction based on the truths $\mu \leq \nu$ and $\pi_{\mathcal{A}}^T \pi_{\mathcal{B}} \leq 1$. There, we have

$$
\omega_2 \geq -(\hat{\Gamma}_1 \eta^2 + \hat{\Gamma}_2 \eta - \hat{\Gamma}_3) \eta, \tag{39}
$$

where

$$
\begin{aligned}
\hat{\Gamma}_1 &= n^{\frac{3}{2}} \kappa_1 \kappa_2 \kappa_3 \delta_{\mathcal{A}2} \delta_{\mathcal{B}2} (1 - \pi_{\mathcal{A}}^T \pi_{\mathcal{B}}) \frac{1}{\mu^3} \\
&\quad + n^{\frac{3}{2}} \kappa_1 \kappa_3 \delta_{\mathcal{AB}} \delta_{\mathcal{B}2} \pi_{\mathcal{A}}^T \pi_{\mathcal{B}} \frac{1}{\mu^3} \\
&\quad + \sqrt{n} \kappa_1 \kappa_3 \delta_{\mathcal{AB}} \delta_{\mathcal{B}2} \pi_{\mathcal{A}}^T \pi_{\mathcal{B}} \alpha \frac{1}{\mu^2 \nu} \\
&\quad + n^{\frac{3}{2}} \kappa_1 \kappa_3 \delta_{\mathcal{AB}} \delta_{\mathcal{B}2} \pi_{\mathcal{A}}^T \pi_{\mathcal{B}} \frac{1}{\mu^3} \\
&\quad + n^{\frac{3}{2}} \kappa_1 \kappa_3 \delta_{\mathcal{A}2} \delta_{\mathcal{B}2} (1 - \pi_{\mathcal{A}}^T \pi_{\mathcal{B}}) \frac{1}{\mu^2} \\
&\quad + n^{\frac{3}{2}} \kappa_1 \kappa_2 \kappa_3 \delta_{\mathcal{A}2} \delta_{\mathcal{B}2} \frac{1}{\mu^3} + n^{\frac{3}{2}} \kappa_1 \kappa_3 \delta_{\mathcal{AB}} \delta_{\mathcal{B}2} \frac{1}{\mu^2} \\
&\quad + n^{\frac{1}{2}} \kappa_1 \kappa_3 \pi_{\mathcal{A}}^T \pi_{\mathcal{B}} \delta_{\mathcal{A}2} \delta_{\mathcal{B}2} \frac{1}{\mu^2 \nu} \\
&\quad + n \alpha \kappa_1 \kappa_3 \kappa_4 (\delta_{\mathcal{A}2} - \delta_{\mathcal{AB}}) \delta_{\mathcal{B}2} \frac{1}{\mu^2} \\
&\quad + n^{\frac{3}{2}} \kappa_1 \kappa_2 \delta_{\mathcal{A}2} (1 - \sigma_{\mathcal{B}}) \frac{1}{\mu^2} \\
&\quad + n \alpha \kappa_1 \kappa_3 \kappa_4 (\delta_{\mathcal{AB}} - \delta_{\mathcal{A}2}) \delta_{\mathcal{B}2} \frac{1}{\mu} \\
&\quad + n^{\frac{3}{2}} \kappa_1 \delta_{\mathcal{A}2} (1 - \sigma_{\mathcal{B}}) \pi_{\mathcal{A}}^T \pi_{\mathcal{B}} \frac{1}{\mu^2} \\
&\quad + \sqrt{n} \kappa_1 \delta_{\mathcal{A}2} (1 - \sigma_{\mathcal{B}}) \pi_{\mathcal{A}}^T \pi_{\mathcal{B}} \frac{1}{\mu \nu} \\
&\quad + \alpha \kappa_1 \kappa_3 \kappa_4 \pi_{\mathcal{A}}^T \pi_{\mathcal{B}} (\delta_{\mathcal{A}2} + \delta_{\mathcal{AB}}) \delta_{\mathcal{B}2} \frac{1}{\mu \nu} \\
&\quad + n \kappa_3 \delta_{\mathcal{B}2} (1 - \sigma_{\mathcal{A}}) \frac{1}{\mu^2} + n^{\frac{3}{2}} \kappa_1 \kappa_3 \delta_{\mathcal{A}2} \delta_{\mathcal{B}2} \frac{1}{\mu^3} \\
&\quad + \kappa_3 \delta_{\mathcal{B}2} \pi_{\mathcal{A}}^T \pi_{\mathcal{B}} (1 - \sigma_{\mathcal{A}}) \frac{1}{\mu \nu}, \\
\hat{\Gamma}_2 &= 3 n \alpha \kappa_1 \kappa_2 \kappa_3 \kappa_5 \delta_{\mathcal{A}2} \delta_{\mathcal{B}2} \frac{1}{\mu^2}, \\
\hat{\Gamma}_3 &= -n \frac{1}{\mu} (1 - \sigma_{\mathcal{A}}) (1 - \sigma_{\mathcal{B}}) \\
&\quad - n \alpha \kappa_1 \kappa_2 \kappa_4 (1 - \sigma_{\mathcal{B}}) \frac{1}{\mu} - \alpha \kappa_1 \kappa_5 \pi_{\mathcal{A}}^T \pi_{\mathcal{B}} \delta_{\mathcal{A}2} \frac{1}{\nu}.
\end{aligned} \tag{40}
$$

Finally, it can be obtained that

$$
\begin{aligned}
\det(I_4 - G) \geq &- \eta \{ [(1 - \theta) \Gamma_1 + \theta \hat{\Gamma}_1] \eta^2 \\
&+ [(1 - \theta) \Gamma_2 + \theta \Gamma_2] \eta \\
&- [(1 - \theta) \Gamma_3 + \theta \hat{\Gamma}_3] \} \\
= &-\eta (\Gamma_{\theta,1} \eta^2 + \Gamma_{\theta,2} \eta - \Gamma_{\theta,3}) > 0,
\end{aligned} \tag{41}
$$

where $\Gamma_{\theta,1} = (1-\theta)\Gamma_1 + \theta \hat{\Gamma}_1$, $\Gamma_{\theta,2} = (1-\theta)\Gamma_2 + \theta \hat{\Gamma}_2$, $\Gamma_{\theta,3} = (1-\theta)\Gamma_3 + \theta \hat{\Gamma}_3$. Thus, the result $\eta < \frac{2\Gamma_{\theta,3}}{\Gamma_{\theta,2} + \sqrt{\Gamma_{\theta,2}^2 - \Gamma_{\theta,1}\Gamma_{\theta,3}}}$ can be derived. $\square$

REFERENCES

[1] T. Guo, M. I. Henwood, and M. van Ooijen, "An algorithm for combined heat and power economic dispatch," *IEEE Trans. Power Syst.*, vol. 11, no. 4, pp. 1778–1784, Nov. 1996.

[2] J.-Y. Fan and L. Zhang, "Real-time economic dispatch with line flow and emission constraints using quadratic programming," *IEEE Trans. Power Syst.*, vol. 13, no. 2, pp. 320–325, May 1998.

[3] S. Shao, F. Gao, and J. Wu, "Distributed multi-area intraday economic dispatch using modified critical region projection algorithm," *IEEE Trans. Autom. Sci. Eng.*, vol. 21, no. 2, pp. 2074–2087, Apr. 2024.

[4] D. Kopp, L. Mönch, D. Pabst, and M. Stehli, "Qualification management in wafer fabs: Optimization approach and simulation-based performance assessment," *IEEE Trans. Autom. Sci. Eng.*, vol. 17, no. 1, pp. 475–489, Jan. 2020.

[5] G. Wen, X. Yu, and Z. Liu, "Recent progress on the study of distributed economic dispatch in smart grid: An overview," *Frontiers Inf. Technol. Electron. Eng.*, vol. 22, no. 1, pp. 25–39, Jan. 2021.

[6] Y. Li, J. Wang, R. Wang, W. Gao, Q. Sun, and H. Zhang, "A switched Newton–Raphson-based distributed energy management algorithm for multienergy system under persistent DoS attacks," *IEEE Trans. Autom. Sci. Eng.*, vol. 19, no. 4, pp. 2985–2997, Oct. 2022.

[7] P. Yi, Y. Hong, and F. Liu, "Initialization-free distributed algorithms for optimal resource allocation with feasibility constraints and application to economic dispatch of power systems," *Automatica*, vol. 74, pp. 259–269, Dec. 2016.

[8] A. Cherukuri and J. Cortés, "Initialization-free distributed coordination for economic dispatch under varying loads and generator commitment," *Automatica*, vol. 74, pp. 183–193, Dec. 2016.

[9] L. Bai, M. Ye, C. Sun, and G. Hu, "Distributed economic dispatch control via saddle point dynamics and consensus algorithms," *IEEE Trans. Control Syst. Technol.*, vol. 27, no. 2, pp. 898–905, Mar. 2019.

[10] P. Li, J. Hu, L. Qiu, Y. Zhao, and B. K. Ghosh, "A distributed economic dispatch strategy for power-water networks," *IEEE Trans. Control Netw. Syst.*, vol. 9, no. 1, pp. 356–366, Mar. 2022.

[11] R. Ren, Y. Li, Q. Sun, X. Xie, L. Liu, and D. W. Gao, "Digital twin assisted economic dispatch for energy Internet with information entropy," *IEEE Trans. Automat. Sci. Eng.*, early access, Apr. 12, 2024, doi: 10.1109/TASE.2024.3386358.

[12] Y. Li, B. Huang, J. Dai, D. W. Gao, Q. Sun, and H. Zhang, "Distributed resilient initialization-free Jacobi descent algorithm for constrained optimization against DoS attacks," *IEEE Trans. Autom. Sci. Eng.*, vol. 21, no. 3, pp. 3332–3343, Jul. 2024.

[13] L. Liu and G. Yang, "Distributed fixed-time optimal resource management for microgrids," *IEEE Trans. Autom. Sci. Eng.*, vol. 20, no. 1, pp. 404–412, Jan. 2023.

[14] P. Gong, Q. G. Wang, and C. K. Ahn, "Finite-time distributed optimization in unbalanced multiagent networks: Fractional-order dynamics, disturbance rejection, and chatter avoidance," *IEEE Trans. Autom. Sci. Eng.*, early access, Sep. 4, 2024, doi: 10.1109/TASE.2024.3452472.

[15] M. Doostmohammadian, W. Jiang, M. Liaquat, A. Aghasi, and H. Zarrabi, "Discretized distributed optimization over dynamic digraphs," *IEEE Trans. Autom. Sci. Eng.*, early access, Apr. 4, 2024, doi: 10.1109/TASE.2024.3383894.

[16] Z. Wang, D. Wang, C. Wen, F. Guo, and W. Wang, "Push-based distributed economic dispatch in smart grids over time-varying unbalanced directed graphs," *IEEE Trans. Smart Grid*, vol. 12, no. 4, pp. 3185–3199, Jul. 2021.

[17] W. Liu, P. Zhuang, H. Liang, J. Peng, and Z. Huang, "Distributed economic dispatch in microgrids based on cooperative reinforcement learning," *IEEE Trans. Neural Netw. Learn. Syst.*, vol. 29, no. 6, pp. 2192–2203, Jun. 2018.

[18] W. Chen and T. Li, "Distributed economic dispatch for energy Internet based on multiagent consensus control," *IEEE Trans. Autom. Control*, vol. 66, no. 1, pp. 137–152, Jan. 2021.
[19] H. Pourbabak, J. Luo, T. Chen, and W. Su, "A novel consensus-based distributed algorithm for economic dispatch based on local estimation of power mismatch," *IEEE Trans. Smart Grid*, vol. 9, no. 6, pp. 5930–5942, Nov. 2018.
[20] H. Xing, Y. Mou, M. Fu, and Z. Lin, "Distributed bisection method for economic power dispatch in smart grid," *IEEE Trans. Power Syst.*, vol. 30, no. 6, pp. 3024–3035, Nov. 2015.
[21] R. Wang, Q. Li, B. Zhang, and L. Wang, "Distributed consensus based algorithm for economic dispatch in a microgrid," *IEEE Trans. Smart Grid*, vol. 10, no. 4, pp. 3630–3640, Jul. 2019.
[22] G. Chen and Q. Yang, "An ADMM-based distributed algorithm for economic dispatch in islanded microgrids," *IEEE Trans. Ind. Informat.*, vol. 14, no. 9, pp. 3892–3903, Sep. 2018.
[23] Z. Dong, S. Mao, M. Perc, W. Du, and Y. Tang, "A distributed dynamic event-triggered algorithm with linear convergence rate for the economic dispatch problem," *IEEE Trans. Netw. Sci. Eng.*, vol. 10, no. 1, pp. 500–513, Jan. 2023.
[24] F. Teng, Z. Ban, T. Li, Q. Sun, and Y. Li, "A privacy-preserving distributed economic dispatch method for integrated port microgrid and computing power network," *IEEE Trans. Ind. Informat.*, vol. 20, no. 8, pp. 10103–10112, Aug. 2024.
[25] J. Zhang, K. You, and L. Xie, "Innovation compression for communication-efficient distributed optimization with linear convergence," *IEEE Trans. Autom. Control*, vol. 68, no. 11, pp. 6899–6906, Nov. 2023.
[26] Z. Chen, S. Liang, L. Li, and S. Cheng, "Quantized primal-dual algorithms for network optimization with linear convergence," *IEEE Trans. Autom. Control*, vol. 69, no. 1, pp. 471–478, Jan. 2024.
[27] Y. Yan, Z. Chen, V. Varadharajan, M. J. Hossain, and G. E. Town, "Distributed consensus-based economic dispatch in power grids using the Paillier cryptosystem," *IEEE Trans. Smart Grid*, vol. 12, no. 4, pp. 3493–3502, Jul. 2021.
[28] W. Chen, Z. Wang, Q. Ge, H. Dong, and G.-P. Liu, "Quantized distributed economic dispatch for microgrids: Paillier encryption–decryption scheme," *IEEE Trans. Ind. Informat.*, vol. 20, no. 4, pp. 6552–6562, Apr. 2024.
[29] J. Zhang, K. You, and K. Cai, "Distributed dual gradient tracking for resource allocation in unbalanced networks," *IEEE Trans. Signal Process.*, vol. 68, pp. 2186–2198, 2020.
[30] T. Charalambous, M. G. Rabbat, M. Johansson, and C. N. Hadjicostis, "Distributed finite-time computation of digraph parameters: Left-eigenvector, out-degree and spectrum," *IEEE Trans. Control Netw. Syst.*, vol. 3, no. 2, pp. 137–148, Jun. 2016.
[31] Q. Lü, X. Liao, H. Li, and T. Huang, "Achieving acceleration for distributed economic dispatch in smart grids over directed networks," *IEEE Trans. Netw. Sci. Eng.*, vol. 7, no. 3, pp. 1988–1999, Jul. 2020.
[32] Y. Xu, T. Han, K. Cai, Z. Lin, G. Yan, and M. Fu, "A distributed algorithm for resource allocation over dynamic digraphs," *IEEE Trans. Signal Process.*, vol. 65, no. 10, pp. 2600–2612, May 2017.
[33] T. T. Doan and A. Olshevsky, "On the geometric convergence rate of distributed economic dispatch/demand response in power networks," 2016, *arXiv:1609.06660*.
[34] S. Pu and A. Nedić, "Distributed stochastic gradient tracking methods," *Math. Program.*, vol. 187, pp. 409–457, May 2021.

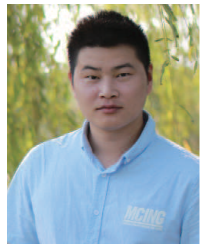

Xiasheng Shi (Member, IEEE) received the B.S. degree in automation from Hefei University of Technology, Hefei, China, in 2014, and the Ph.D. degree in control theory and control engineering from Zhejiang University, Hangzhou, China, in 2020. He is currently a Post-Doctoral Researcher with the School of Artificial Intelligence, Anhui University, Hefei. His research interests include the distributed optimization, control, and estimation.

Changyin Sun (Senior Member, IEEE) received the B.S. degree in applied mathematics from Sichuan University, Chengdu, China, in 1996, and the M.S. and Ph.D. degrees in electrical engineering from Southeast University, Nanjing, China, in 2001 and 2004, respectively.

He is currently a Professor with the School of Artificial Intelligence, Anhui University, Hefei, China. His research interests include intelligent control, flight control, and optimal theory. He is an Associate Editor of IEEE TRANSACTIONS ON NEURAL NETWORKS AND LEARNING SYSTEMS, *Neural Processing Letters*, and IEEE/CAA JOURNAL OF AUTOMATICA SINICA.

Chaoxu Mu (Senior Member, IEEE) received the Ph.D. degree in control science and engineering from the School of Automation, Southeast University, Nanjing, China, in 2012.

She was a Visiting Ph.D. Student with the Royal Melbourne Institute of Technology, Melbourne, VIC, Australia, from 2010 to 2011. Since 2014, she has been a Professor with the School of Electrical and Information Engineering, Tianjin University, Tianjin, China. Her current research interests include nonlinear system control and optimization and adaptive and learning systems.